can be easily measured are necessary to accurately diagnose NASH or CHC.

In recent years, proteomic techniques, including 2-D gel electrophoresis (2-DE), have been commonly used to explore novel biomarkers. However, traditional 2-DE-based proteomic approaches are tedious and have several limitations, including reduced sensitivity and lack of quantitative results. Isotope-coded affinity tagging (ICAT) and isotope tagging for relative and absolute quantitation (iTRAQ) are the most commonly used chemical isotope labeling methods and can be used to address many of the limitations of 2-DE. In this report, we examined a novel stable isotope labeling method, the 2-nitrobenzenesulfenyl (NBS) labeling method developed by Kuyama *et al.*[7] The NBS labeling method is based on the specific binding reaction of the NBS reagent to tryptophan residues within a protein, and the 6-Da mass difference between [^{12}C]-NBS-labeled and [^{13}C]-NBS-labeled peptides generates a mass signature for all tryptophan-containing peptides.[7,8]

Here, we explored novel oxidative stress marker candidates using the NBS labeling method and identified four candidate oxidative stress markers in human primary hepatocytes including MnSOD. Furthermore, we verified the clinical significance of MnSOD as a diagnostic marker for NASH.

METHODS

Chemicals and materials

THE ^{13}CNBS® STABLE isotope labeling kit-N was purchased from Shimadzu Biotech (Kyoto, Japan). Human primary hepatocytes (a monolayer of human long-term hepatocytes), which were isolated from a 77-year-old woman, were purchased from Biopredic International (Rennes, France). 4-Hydroxycinnamic acid (CHCA) was obtained from Bruker Daltonics (Bremen, Germany) and 3-hydroxy-4-nitrobenzoic acid (3H4NBA) was purchased from Sigma Chemical (St Louis, MO, USA). Sequencing-grade modified trypsin was from Promega (Madison, WI, USA), and the protease inhibitor cocktail set III was from Calbiochem (Darmstadt, Germany).

Cell culture, NBS labeling and identification of NBS-labeled peptides

Human primary hepatocytes were cultured in a long-term culture medium.[9] Confluent human primary hepatocytes (~2×10^6 cells/12.5 cm^2 flask) were incubated for 24 h with phosphate buffered saline (PBS) or 200 μM hydrogen peroxide (H_2O_2).[10,11] Cells were washed and homogenized in 50 mM phosphate buffer, pH 8.0, containing 1% protease inhibitor cocktail set III. The NBS labeling was performed as previously described.[12,13] Briefly, both cell lysates (100 μg) treated with PBS or H_2O_2 were labeled with [^{12}C]- or [^{13}C]-NBS under acidic conditions, respectively. After labeling, the two respective conditioned protein mixtures were denatured with urea and reduced with tris(2-carboxyethyl)phosphine (TCEP) followed by alkylation with iodoacetamide. NBS-labeled proteins were digested with trypsin and eluted through phenyl sepharose using a stepwise gradient of increasing acetonitrile (10%, 15%, 20%, 25%, 30%, 35%, 40%, 45% and 50%) containing 0.1% trifluoro acetate. Next, the NBS-labeled peptides were ionized by a combined application of CHCA and 3H4NBA as described.[14,15] The mass spectral data were obtained by MALDI-TOF-TOF-MS, Autoflex II TOF/TOF (Bruker Daltonics) in positive-ion and reflectron mode. Pairs of peaks with a 6-Da difference were identified by MS/MS ion searching using tandem MS. The data set from the MS/MS ion was analyzed using the database search engine, Mascot (www.matrixscience.com), to find the closest match with known proteins/peptides in the database from the Swiss-Prot website.

Western blot analysis

Equal amounts of cell lysates from human primary hepatocytes (4 μg) were run on sodium dodecylsulfate polyacrylamide gels and electroblotted onto polyvinylidene fluoride membranes. The blots were probed with anti-cytochrome *c* oxidase VIb isoform 1 (anti-COX6B), anti-liver carboxylesterase 1 (anti-CES1), anti-carbamoyl-phosphate synthase [ammonia] mitochondrial 1 (anti-CPS1) and anti-MnSOD antibodies. After incubating the membrane with the appropriate horseradish peroxidase-conjugated secondary antibody, the reactivity was visualized using an ECL chemiluminescent detection kit (GE Healthcare Biosciences, Tokyo, Japan).

Real-time reverse transcription polymerase chain reaction (RT–PCR)

Total RNA was extracted from cells using ISOGEN (Nippon Gene, Toyama, Japan) according to the manufacturer's instructions. Samples were reverse-transcribed using the PrimeScript RT reagent Kit (TAKARA Bio, Shiga, Japan). Synthesized cDNA was amplified using SYBR Premix Ex Taq II (TAKARA Bio) and analyzed by StepOnePlus Real-Time PCR Systems and StepOne

Table 1 Identification and quantification of 2-nitrobenzenesulfenyl-labeled peak pairs

Accession no.	Protein name	Peak pairs (^{12}C–^{13}C, m/z)	Identified sequences
P14853	Cytochrome *c* oxidase subunit VIb isoform 1	1705–1711	NC**W**QNYLDFHR
P23141	Liver carboxylesterase 1 precursor	1783–1789	FTPPQPAEP**W**SFVK
P31327	Carbamoyl-phosphate synthase [ammonia], mitochondrial precursor	1902–1908	GAEVHLVP**W**NHDFTK
P04179	Superoxide dismutase [Mn], mitochondrial precursor	2790–2796	FNGGGHINHSIF**W**TNLSPNGGGEPK

Bold and underlined characters highlight the tryptophan (W) residues in the identified peptide sequences.

Software ver. 2.0 (Applied Biosystems, Foster City, CA, USA). The cycle conditions were as follows: one cycle at 95°C for 30 s followed by 35 cycles each at 95°C for 5 s and 60°C for 34 s. To normalize the amount of total RNA present in each reaction, the glyceraldehydes 3-phosphate dehydrogenase (GAPDH) gene was used as an internal standard.

Serum samples and MnSOD enzyme-linked immunosorbent assay (ELISA)

Serum samples were obtained from 20 healthy subjects, 15 simple steatosis (SS) patients and 29 NASH patients after a thorough clinical evaluation. Signed informed consent was obtained from each patient. The patients were diagnosed at University Hospital, Kyoto Prefectural University of Medicine (Kyoto, Japan) and Kagoshima University (Kagoshima, Japan). The study protocol was approved by the Ethics Committee of the Kagoshima University Hospital, the Kyoto Prefectural University of Medicine and the Miyazaki Prefectural Industrial Support Foundation. Serum MnSOD levels were measured by a Human Superoxide Dismutase 2 ELISA (AbFRONTIER, Seoul, Korea).

Statistical analysis

Differences among three groups were evaluated using Kruskal–Wallis test followed by Dunn's multiple comparison test. Correlation coefficients were calculated by Spearman's rank correlation analysis. A receiver-operator curve (ROC) was constructed by plotting the sensitivity and specificity (100 – specificity) for each value.

RESULTS

THE NBS-LABELED peptides from human primary hepatocytes were analyzed by MALDI-TOF/MS, and 73 pairs of peaks with 6-Da differences were detected in all mass spectra. Among these pairs of peaks, 44 pairs had a greater signal intensity in the H_2O_2-loaded sample compared to the PBS-loaded sample (data not shown). Among these 44 pairs of peaks, four peak pairs, m/z 1705–1711, m/z 1783–1789, m/z 1902–1908 and m/z 2790–2796, were identified as COX6B, CES1, CPS1 and superoxide dismutase (Mn), mitochondrial (MnSOD), respectively, by MS/MS ion searching (Table 1). The MS spectrum of the m/z 2790–2796 pair and the MS/MS spectrum of 2796 m/z ([^{13}C]-NBS labeled; MnSOD) are shown in Figure 1(a,b), respectively. Western blotting and real-time RT-PCR revealed that the protein and mRNA expression for each of these molecules increased in human primary hepatocytes after H_2O_2 loading (Fig. 1c–e).

Figure 1 Typical MS spectrum and MS/MS spectra from a proteomic analysis. (a) MALDI-TOF/MS spectra of a pair of peaks, 2790–2796 m/z, and the relative intensities of the [^{13}C]-2-nitrobenzenesulfenyl (NBS)-labeled peak compared to the [^{12}C]-NBS-labeled peak. Relative intensities are the means of two independent values analyzed by Autoflex II TOF/TOF. (b) MS/MS spectra of 2796 m/z ([13C]-NBS-labeled). From the detected MS/MS spectra, superoxide dismutase (Mn) mitochondrial was identified. (c) Equal amounts of cell extracts (4 μg) from human primary hepatocytes loaded with 200 μM hydrogen peroxide (H_2O_2) for 24 h were separated by sodium dodecylsulfate polyacrylamide gel electrophoresis and then immunoblotted with cytochrome *c* oxidase VIb isoform 1 (COX6B)-, liver carboxylesterase 1 (CES1)-, carbamoyl-phosphate synthase (ammonia), mitochondrial 1 (CPS1)-, superoxide dismutase [Mn], mitochondrial (MnSOD)- or β-actin-specific antibodies. (d) Quantitative representation of the western blot data. The results have been normalized to β-actin levels and are expressed as the levels relative to untreated cells. The data are the means of duplicate cultures. (e) The mRNA expression levels of COX6B, CES1, CPS1, MnSOD and glyceraldehyde 3-phosphate dehydrogenase (GAPDH) were measured by real-time polymerase chain reaction. The results have been normalized to GAPDH and are expressed as the levels relative to untreated cells. The data are the means of duplicate cultures. PBS, phosphate buffered saline.

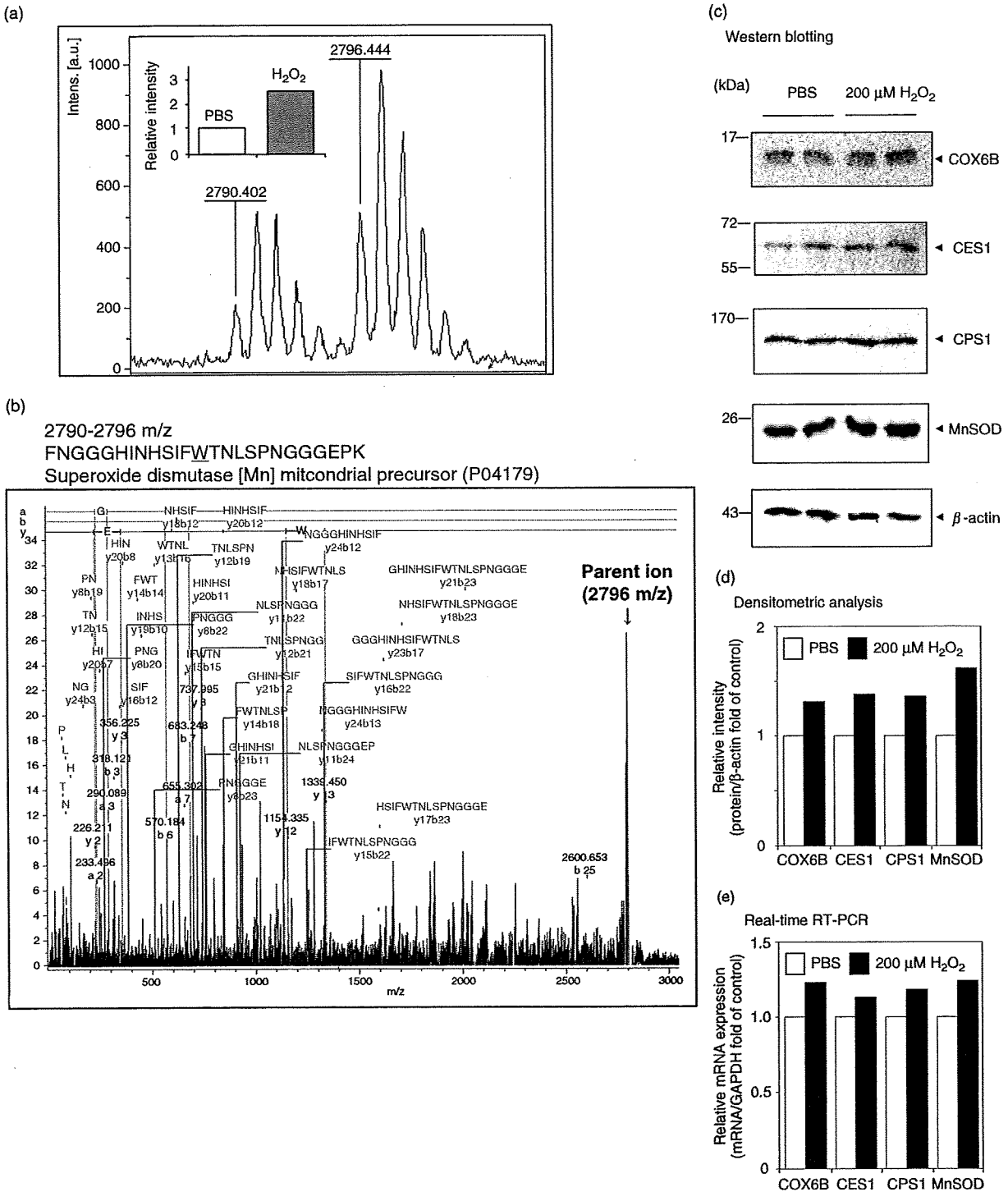

Table 2 Characteristics of study subjects

	Simple steatosis ($n = 15$)	NASH ($n = 29$)	*P*-value
Age (years)	43.2 ± 14.0	60.8 ± 14.9	**<0.001**
Sex (male/female)	11/4	11/18	**<0.05**
Height (cm)	162.5 ± 11.2	156.5 ± 8.7 (28)	0.05
Bodyweight (kg)	69.3 ± 11.8	69.2 ± 15.2 (28)	0.58
BMI (kg/m^2)	26.3 ± 3.6	28.1 ± 4.4 (28)	0.23
Diabetes (yes/no)	5/10	13/15 (28)	0.52
Hyperlipidemia (yes/no)	10/5	16/12 (28)	0.74
Hypertension (yes/no)	4/11	10/18 (28)	0.74
Hb (g/dL)	15.1 ± 1.8	14.4 ± 1.5	0.07
Plt (×10^4/μL)	23.8 ± 7.5	18.8 ± 7.0	**<0.05**
AST (IU/L)	41.6 ± 20.2	69.4 ± 46.5	**<0.05**
ALT (IU/L)	83.1 ± 53.1	94.6 ± 96.0	0.89
γ-GTP (U/L)	75.3 ± 52.4	155.6 ± 303.1	0.40
ChE (IU/L)	417.9 ± 97.5	352.8 ± 135.5	**<0.05**
γ-Glob (g/dL)	1.27 ± 0.40	1.50 ± 0.44 (24)	0.06
Total cholesterol (mg/dL)	209.2 ± 45.8	204.8 ± 52.1	0.97
Triglyceride (mg/dL)	168.3 ± 65.8	184.8 ± 168.3	0.45
BS (mg/dL)	119.1 ± 48.5	112.3 ± 34.3	0.61
Ferritin (mg/dL)	190.0 ± 112.7 (14)	239.8 ± 234.3 (22)	0.75

Values represent means ± standard deviation for the indicated number of subjects. Significant differences between the mean values ($P < 0.05$) were assessed by Fisher's exact probability test (sex, diabetes, hyperlipidemia and hypertension) or Mann–Whitney's *U*-test (other items).
Values in parentheses indicate the number of samples. Bold characters highlight statistically significant *P*-values.
ALT, alanine aminotransferase; AST, aspartate aminotransferase; BMI, body mass index; BS, blood sugar; ChE, choline esterase; γ-Glob, γ-globulin; γ-GTP, γ-glutamyl transpeptidase; Hb, hemoglobin; NASH, non-alcoholic steatohepatitis; Plt, platelet count.

The clinical characteristics of the SS and NASH groups were not significantly different except for the average age, platelet count (Plt), aspartate aminotransferase (AST) and choline esterase (ChE) (Table 2). We examined the serum MnSOD levels in healthy subjects ($n = 20$), SS patients ($n = 15$) and NASH patients ($n = 29$). There were no significant differences in MnSOD serum levels between healthy subjects and SS patients (Fig. 2a). In contrast, NASH patients had significantly higher serum MnSOD levels than both healthy subjects and SS patients (Fig. 2a). In addition, as shown in Figure 2(b), the serum levels of MnSOD tended to increase in parallel with the fibrosis stage. In contrast, there was no correlation between the levels of MnSOD and the activity grade of NASH (Fig. 2c). ROC of MnSOD levels were constructed to distinguish NASH (29 patients) from SS (15 patients) (Fig. 2d). The serum MnSOD threshold level that was used to predict NASH was calculated to be 71.8 ng/mL. At this threshold, the sensitivity was 69.0% and the specificity was 80.0%. The area under the ROC (AUC) for serum MnSOD levels was 0.760 ($P = 0.010$). The ROC curves for Plt, AST and ChE, which were significantly different between SS and NASH (Table 2), were also constructed. As a result, the AUC (*P*-value, threshold, sensitivity [%], specificity [%]) for Plt, serum AST and ChE were 0.733 (0.012, 19.4, 65.5, 86.7), 0.726 (0.015, 42.0, 65.5, 73.3) and 0.687 (0.044, 317.5, 48.3, 86.7), respectively.

DISCUSSION

IN THIS REPORT, we used the NBS labeling method to identify novel oxidative stress markers in hepatocytes that can be used as diagnostic markers for NASH and identified four candidate markers, COX6B, CES1, CPS1 and MnSOD, that were upregulated with H_2O_2 loading (Table 1, Fig. 1). Several recent studies have reported novel approaches that combine the NBS labeling method with 2-DE, high-performance liquid chromatography (HPLC) and lectin column chromatographic techniques.[13–16] In our present study, we identified only four proteins, indicating that it may be necessary to modify the current method by 2-DE and column chromatographic techniques to identify additional NBS-

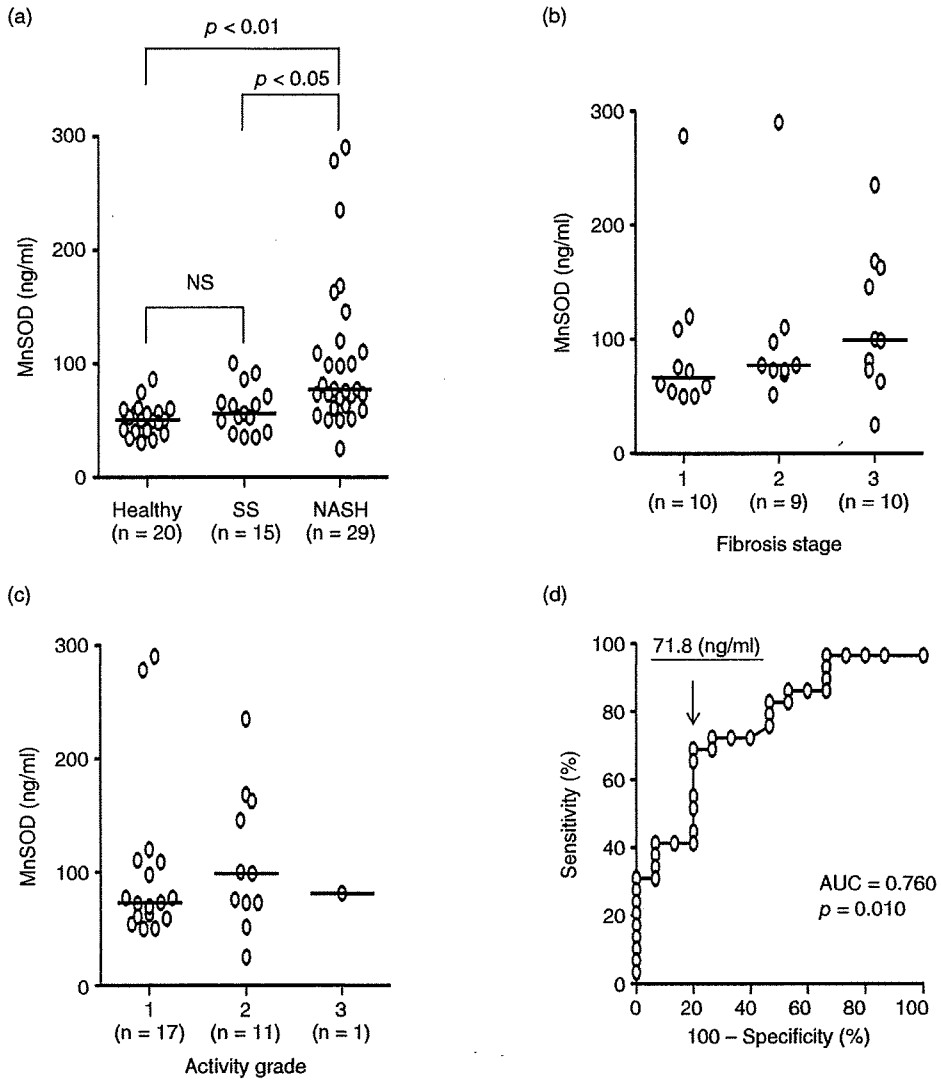

Figure 2 Clinical significance of serum MnSOD levels. (a) Serum MnSOD levels in healthy subjects and patients with SS or non-alcoholic steatohepatitis (NASH). Serum MnSOD levels were measured by enzyme-linked immunosorbent assay. (b) Comparison between serum MnSOD levels and the fibrosis stage in SS and NASH patients. (c) Comparison between serum MnSOD levels and the activity grade in SS and NASH patients. (d) Receiver–operator curve for MnSOD. The differences among three groups were evaluated using Kruskal–Wallis test followed by Dunn's multiple comparison test. Correlation coefficients were calculated by Spearman's rank correlation analysis. Bars indicate the median in the respective groups. AUC, area under the curve.

labeled peptides. In addition, further studies are needed to identify novel biomarkers by other proteomic techniques using serum samples from SS and NASH patients.

COX6B, CPS1 and MnSOD are mitochondrial proteins, and therefore may be indicators of mitochondrial disorders that are induced by oxidative stress. CPS1 is expressed primarily in the liver and small intestine and is involved in the urea cycle.[17] In galactosamine-induced rat acute hepatitis, plasma concentrations of CPS1 increase up to approximately 100-fold for 24 h after treatment.[18] This may indicate that secreted CPS1 is a serum marker for acute hepatitis. CES1, which is responsible for detoxification of exogenous compounds such

as esters, amides and thioesters, is also known to exist in the serum. Therefore, CES1, like CPS1, may be a serum oxidative stress marker.[19,20] Additional studies are needed to further evaluate the serum levels of these identified proteins.

MnSOD primarily exists in the mitochondrial matrix and eliminates reactive oxygen species (ROS) by catalyzing the dismutation of superoxide radicals and hydrogen peroxide.[19] Furthermore, MnSOD expression was previously shown to increase after exposure to hydrogen peroxide in rat hepatocytes.[21] In addition, obese mice were previously reported to have increased hepatic H_2O_2 levels and necrosis following an imbalance between increased MnSOD, which forms H_2O_2, and decreased glutathione activity, which detoxifies H_2O_2.[22] We found that MnSOD is potentially a novel diagnostic marker of NASH that can be used to distinguish between SS and NASH. One of the mechanisms contributing to increased MnSOD serum levels in NASH might be the discharge of MnSOD from necrotic hepatocytes. On the other hand, in the liver, several pro-inflammatory cytokines, such as tumor necrosis factor-α, interleukin-6 and interleukin-1β can act as common inducers of NASH.[23,24] Such pro-inflammatory cytokines have been shown to induce MnSOD expression in liver tissues.[25] Furthermore, pro-inflammatory cytokines induced the expression and secretion of MnSOD in several cancer cell lines including hepatoma cells.[26,27] In our present study, the origin of MnSOD produced in NASH and the precise mechanism of increased serum levels of MnSOD in NASH patients remain unclear. However, these reports may partially support the mechanism of MnSOD production in NASH. Further elucidation is necessary to clarify the mechanism of MnSOD expression and production in NASH.

Several reports have shown a relationship between the enzymatic activity of MnSOD and non-alcoholic fatty liver disease, NASH, liver cirrhosis and hepatocellular carcinoma.[28–31] Ono *et al.* showed that MnSOD serum levels were significantly increased in patients with primary biliary cirrhosis compared to patients with other liver diseases.[32] However, the serum protein levels of MnSOD in liver diseases have not been fully evaluated. In addition, the enzymatic activity of serum MnSOD was not different among the three groups and this activity did not correlate with serum MnSOD levels in our study (data not shown). The reasons for these results are unclear. However, as shown in Figure 2(b), serum MnSOD levels increased in parallel with the stage of fibrosis in NASH. The increase in serum MnSOD levels also significantly correlated with the serum AST levels (data not shown). These results indicate that serum MnSOD might be a biomarker that reflects hepatitic and fibrotic pathology. In addition, although MnSOD levels should increase in patients with other diseases including CHC, ROC analysis revealed that serum MnSOD may be a more sensitive biomarker than Plt, AST and ChE. We concluded that serum MnSOD is a useful biomarker that can distinguish SS and NASH.

ACKNOWLEDGMENTS

THIS WORK WAS supported in part by Grants-in-Aid for Scientific Research (C) from the Japan Society for the Promotion of Science (JSPS), Research for Promoting Technological Seeds (A) from the Japan Science and Technology Agency (JST), the Collaboration of Regional Entities for the Advancement of Technological Excellence (CREATE) from the JST, and a Grant-in-Aid (Research on Hepatitis and BSE) from the Ministry of Health, Labor and Welfare of Japan.

REFERENCES

1 Leclercq IA, Farrell GC, Field J, Bell DR, Gonzalez FJ, Robertson GR. CYP2E1 and CYP4A as microsomal catalysts of lipid peroxides in murine nonalcoholic steatohepatitis. *J Clin Invest* 2000; 105: 1067–75.
2 Piccoli C, Scrima R, D'Aprile A *et al.* Mitochondrial dysfunction in hepatitis C virus infection. *Biochim Biophys Acta* 2006; 1757: 1429–37.
3 Perez-Carreras M, Del Hoyo P, Martin MA *et al.* Defective hepatic mitochondrial respiratory chain in patients with nonalcoholic steatohepatitis. *Hepatology* 2003; 38: 999–1007.
4 Wu LL, Chiou CC, Chang PY, Wu JT. Urinary 8-OHdG: a marker of oxidative stress to DNA and a risk factor for cancer, atherosclerosis and diabetics. *Clin Chim Acta* 2004; 339: 1–9.
5 Fujii J, Taniguchi N. Phorbol ester induces manganese-superoxide dismutase in tumor necrsis factor-resistant cells. *J Biol Chem* 1991; 266: 23142–6.
6 Nishinaka Y, Masutani H, Nakamura H, Yodoi J. Regulatory roles of thioredoxin in oxidative stress-induced cellular responses. *Redox Rep* 2001; 6: 289–95.
7 Kuyama H, Watanabe M, Toda C, Ando E, Tanaka K, Nishimura O. An approach to quantitative proteome analysis by labeling tryptophan residues. *Rapid Commun Mass Spectrom* 2003; 17: 1642–50.
8 Matsuo E, Toda C, Watanabe M *et al.* Improved 2-nitrobenzenesulfenyl method: optimization of the protocol and improved enrichment for labeled peptides. *Rapid Commun Mass Spectrom* 2006; 20: 31–8.

9 Lanford RE, Carey KD, Estlack LE, Smith GC, Hay RV. Analysis of plasma protein and lipoprotein synthesis in long-term primary cultures of baboon hepatocytes maintained in serum-free medium. *In Vitro Cell Dev Biol* 1989; 25: 174–82.
10 Rosseland CM, Wierod L, Oksvold MP *et al.* Cytoplasmic retention of peroxide-activated ERK provides survival in primary cultures of rat hepatocytes. *Hepatology* 2005; 42: 200–7.
11 Conde de la Rosa L, Schoemaker MH, Vrenken TE *et al.* Superoxide anions and hydrogen peroxide induce hepatocyte death by different mechanisms: involvement of JNK and ERK MAP kinases. *J Hepatol* 2006; 44: 918–29.
12 Matsuo E, Toda C, Watanabe M *et al.* Selective detection of 2-nitrobenzenesulfenyl-labeled peptides by matrix-assisted laser desorption/ionization-time of flight mass spectrometry using a novel matrix. *Proteomics* 2006; 6: 2042–9.
13 Sumida Y, Nakashima T, Yoh T *et al.* Serum thioredoxin levels as a predictor of steatohepatitis in patients with non-alcoholic fatty liver disease. *J Hepatol* 2003; 38: 32–8.
14 Ou K, Kesuma D, Ganesan K *et al.* Quantitative profiling of drug-associated proteomic alterations by combined 2-nitrobenzenesulfenyl chloride (NBS) isotope labeling and 2DE/MS identification. *J Proteome Res* 2006; 5: 2194–206.
15 Iida T, Kuyama H, Watanabe M *et al.* Rapid and efficient MALDI-TOF MS peak detection of 2-nitrobenzenesulfenyl-labeled peptides using the combination of HPLC and an automatic spotting apparatus. *J Biomol Tech* 2006; 17: 333–41.
16 Ueda K, Katagiri T, Shimada T *et al.* Comparative profiling of serum glycoproteome by sequential purification of glycoproteins and 2-nitrobenzensulfenyl (NBS) stable isotope labeling: a new approach for the novel biomarker discovery for cancer. *J Proteome Res* 2007; 6: 3475–83.
17 Pearson DL, Dawling S, Walsh WF *et al.* Neonatal pulmonary hypertension–urea-cycle intermediates, nitric oxide production, and carbamoyl-phosphate synthetase function. *N Engl J Med* 2001; 344: 1832–8.
18 Ozaki M, Terada K, Kanazawa M, Fujiyama S, Tomita K, Mori M. Enzyme-linked immunosorbent assay of carbamoylphosphate synthethase 1: plasma enzyme in rat experimental hepatitis and its clearance. *Enzyme Protein* 1994–1995; 48: 213–21.
19 Munger JS, Shi GP, Mark EA, Chin DT, Gerard C, Chapman HA. A serine esterase released by human alveolar macrophages is closely related to liver microsomal carboxylesterases. *J Biol Chem* 1991; 266: 18832–8.
20 Yan B, Yang D, Bullock P, Parkinson A. Rat serum carboxylesterase. Cloning, expression, regulation, and evidence of secretion from liver. *J Biol Chem* 1995; 270: 19128–34.
21 Kurobe N, Inagaki T, Kato K. Sensitive enzyme immunoassay for Mn superoxide dismutase. *Clin Chim Acta* 1990; 192: 171–9.
22 Rohrdanz E, Kahl R. Alterations of antioxidant enzyme expression in response to hydrogen peroxide. *Free Radic Biol Med* 1998; 24: 27–38.
23 Robin MA, Demeilliers C, Sutton A *et al.* Alcohol increases tumor necrosis factor a and decreases nuclear factor kB to activate hepatic apoptosis in genetically obese mice. *Hepatology* 2005; 42: 1280–90.
24 Hotamisligil GS. Inflammation and metabolic disorders. *Nature* 2006; 444: 860–7.
25 Shoelson SE, Lee J, Goldfine AB. Inflammation and insulin resistance. *J Clin Invest* 2006; 116: 1793–801.
26 Sato M, Sasaki M, Hojo H. Antioxidative roles of metallothionein and manganese superoxide dismutase induced by tumor necrosis factor-α and interleukin-6. *Arch Biochem Biophys* 1995; 316: 738–44.
27 Ono M, Kohda H, Kawaguchi T *et al.* Induction of Mn-superoxide dismutase by tumor necrosis factor, interleukin-1 and interleukin-6 in human hepatoma cells. *Biochem Biophys Res Commun* 1992; 182: 1100–7.
28 Nakata T, Suzuki K, Fujii J, Ishikawa M, Taniguchi N. Induction and release of manganese superoxide dismutase from mitochondria of human umbilical vein endothelial cells by tumor necrosis factor-α and interleukin-1β. *Int J Cancer* 1993; 55: 646–50.
29 Videla LA, Rodrigo R, Orellana M *et al.* Oxidative stress-related parameters in the liver of non-alcoholic fatty liver disease patients. *Clin Sci* 2004; 106: 261–8.
30 Clemente C, Elba S, Buongiorno G *et al.* Manganese superoxide dismutase activity and incidence of hepatocellular carcinoma in patients with Child–Pugh class A liver cirrhosis: 7-year follow-up study. *Liver Int* 2007; 27: 791–7.
31 Perlemuter G, Davit-Spraul A, Cosson C *et al.* Increase in liver antioxidant enzyme activities in non-alcoholic fatty liver disease. *Liver Int* 2005; 25: 946–53.
32 Ono M, Sekiya C, Ohhira M *et al.* Elevated level of serum Mn-superoxide dismutase in patients with primary biliary cirrhosis: possible involvement of free radicals in the pathogenesis in primary biliary cirrhosis. *J Lab Clin Med* 1991; 118: 476–83.

J Gastroenterol (2010) 45:459–467
DOI 10.1007/s00535-009-0160-5

ORIGINAL ARTICLE—LIVER, PANCREAS, AND BILIARY TRACT

The complement component C3a fragment is a potential biomarker for hepatitis C virus-related hepatocellular carcinoma

Shuji Kanmura · Hirofumi Uto · Yuko Sato · Koutarou Kumagai · Fumisato Sasaki · Akihiro Moriuchi · Makoto Oketani · Akio Ido · Kenji Nagata · Katsuhiro Hayashi · Sherri O. Stuver · Hirohito Tsubouchi

Received: 1 July 2009 / Accepted: 28 October 2009 / Published online: 9 December 2009

Abstract
Background Hepatocellular carcinoma (HCC) has a high mortality rate, and early detection of HCC improves patient survival. However, the molecular diagnostic markers for early HCC have not been fully elucidated. The aim of this study was to identify novel diagnostic markers for HCC.
Methods Serum protein profiles of 45 hepatitis C virus infection (HCV)-related HCC patients (HCV-HCC) were compared to 42 HCV-related chronic liver disease patients without HCC (HCV-CLD) and 21 healthy volunteers using the ProteinChip SELDI system. One of the identified proteins was evaluated as a diagnostic marker for HCC in patients with HCV.
Results Five protein peaks (4067, 4470, 7564, 7929, and 8130 m/z) had p-values less than 1×10^{-7} and were significantly increased in the sera of HCV-HCC patients compared to HCV-CLD patients and healthy volunteers. Among these proteins, an 8130 m/z peak was the most differentially expressed and identified as the complement component 3a (C3a) fragment. For HCV-HCC and HCV-CLD, the relative intensity of this C3a fragment had the best area under the ROC curve [0.70], followed by des-γ-carboxy prothrombin (DCP) [0.68], lectin-bound alpha fetoprotein (AFP-L3) [0.58] and AFP [0.53] for HCC. A combined analysis of the C3a fragment, AFP and DCP led to a 98% positive identification rate. In addition, the measurable C3a fragment in some HCC patients was not only significantly higher in the year of HCC onset compared to the pre-onset year, but also decreased after treatment.
Conclusions The 8130 m/z C3a fragment is a potential marker for the early detection of HCV-related HCC.

Keywords Hepatocellular carcinoma · Complement component C3a · Serum proteomics · Serum biomarkers · Proteinchip SELDI system · Hepatitis C virus

S. Kanmura · H. Uto (✉) · K. Kumagai · F. Sasaki · A. Moriuchi · M. Oketani · A. Ido · H. Tsubouchi
Digestive Disease and Life-style Related Disease Health Research, Human and Environmental Sciences, Kagoshima University Graduate School of Medical and Dental Sciences, 8-35-1 Sakuragaoka, Kagoshima 890-8520, Japan
e-mail: hirouto@m2.kufm.kagoshima-u.ac.jp

Y. Sato
Miyazaki Prefectual Industrial Support Foundation, Miyazaki, Japan

K. Nagata
Division of Gastroenterology and Hematology, Internal Medicine, Faculty of Medicine, University of Miyazaki, Miyazaki, Japan

K. Hayashi
Faculty of Medicine, Center for Medical Education, University of Miyazaki, Miyazaki, Japan

S. O. Stuver
Department of Epidemiology, Boston University School of Public Health, Boston, MA, USA

S. O. Stuver
Department of Epidemiology, Harvard School of Public Health, Boston, MA, USA

Introduction

Hepatocellular carcinoma (HCC) is reportedly the third most frequent cause of global cancer-related deaths, and the incidence of HCC is increasing worldwide [1, 2]. The clearly established risk factor for HCC is chronic hepatitis C virus (HCV) infection [3].

To date, both ultrasonography and serum tumor markers such as the alpha fetoprotein (AFP), and des-γ-carboxy prothrombin (DCP) assay are the principle methods for screening and detecting HCC. Routine screening is the best method to detect early HCC and improve patient survival; however, elevated serum AFP and DCP levels have insufficient sensitivity and specificity, respectively. The sensitivity and specificity of serum elevated AFP levels were reported to range from 39–64% and 76–91%, while those of the serum elevated DCP levels were 41–77% and 72–98%, respectively [4–9]. In addition, it was recently reported that only a small percentage of small HCC tumors were diagnosed based on AFP and DCP [6, 10]. The lens culinaris agglutinin-reactive fraction of AFP (lectin-bound AFP or AFP-L3) has been reported to be elevated in the serum of HCC patients. Although AFP-L3 has a high range of specificity for detecting HCC, the sensitivity is low [11, 12]. The ability to detect early HCC, prior to the onset of clinical symptoms, leads to curative treatment and significantly improves the disease prognosis. Thus, additional biochemical markers are necessary for the specific detection of early HCC.

Serum profiling using a proteomic approach is thought to be a useful technique to detect or predict early HCC in chronic liver disease patients. Studies using the ProteinChip SELDI system, which is a powerful tool to discover new biomarkers, have shown that this method may be successfully used to diagnose HCC. Zinkin et al. [13], Schwegler et al. [14] and our research group [15] previously detected early HCC using the profile of several protein peaks that were identified by the ProteinChip SELDI system. Paradis et al. [16] reported the highest discriminating peak (8900 Da), which was identified as the V10 fragment of vitronectin. Furthermore, Lee et al. [17] described complement 3a, which had a molecular weight of approximately 8900 Da, as a novel marker of HCC. Therefore, using this proteomic approach to identify specific proteins may not only help establish simple methods to detect HCC, but also further our understanding of the molecular mechanisms of hepatocarcinogenesis and facilitate the development of novel cancer therapies. Therefore, this study assessed and compared the protein expression profiles in the sera of HCC patients in order to identify a more useful biomarker of HCC-associated HCV infection using proteomic approach.

Materials and methods

Samples

Eighty-seven patients [45 HCC patients and 42 patients with chronic liver diseases without HCC (CLD)] with HCV infection were selected to participate in this study (Table 1). These patients provided informed consent. Serum samples were collected by the Faculty of Medicine, University of Miyazaki (Miyazaki, Japan), and some patients were in a hyperendemic HCV area with a cohort study in Miyazaki [18]. The sera of all patients with and without HCC, which was confirmed by abdominal ultrasonography or computed tomography, were obtained prior to treatment. All of the sera samples from HCV-infected patients were analyzed in a previous study [15]. In addition, sera from 10 HCV-HCC patients who were diagnosed with HCC within 1 or 2 years and sera from five patients who had received radiofrequency ablation (RFA), percutaneous ethanol injection therapy (PEIT) and/or transarterial chemoembolization (TACE) for HCC were collected through a cohort study in Miyazaki. We also analyzed the sera of 21 healthy volunteers without HCC as controls. After freezing and thawing once, all samples were separated into 50–100 μl aliquots and refrozen at −80°C. The study protocol was approved by the Ethics Committee of the Faculty of Medicine, University of Miyazaki, Kagoshima University Graduate School of Medical and Dental Sciences, and Harvard School of Public Health and Boston University School of Public Health.

Table 1 Patient characteristics

	HCC[a]	CLD[b]	*p* value
Patients (male/female)	45 (40/5)	42 (40/2)	–
Age	73.6 [63–85]	61.8 [41–83]	<0.0001
PLT[c] ($\times 10^4$/ul)	12.5 ± 5.8	8.4 ± 4.6	0.001
Albumin (g/dl)	3.8 ± 0.8	4.2 ± 1.6	0.8
ALT[d] (IU/l)	57.7 ± 28.3	52.8 ± 37.5	0.7
AFP[e] (ng/ml)	311 ± 1144	51.6 ± 36.1 (38)	0.008
DCP[f] (mAU/ml)	235 ± 605 (44)	37.1 ± 59.8 (39)	<0.0001
HA[g] (ng/ml)	388 ± 446 (40)	280 ± 272 (27)	0.6
Diameter of HCC (mm)	23.2 [10–40]	–	–
TNM stage[h] (I/II/III/IV)	24/18/3/0	–	–

Data are shown as the means ± SD or means [range] (numbers)

[a] Hepatocellular carcinoma

[b] Chronic liver disease

[c] Platelet counts

[d] Alanine aminotransferase

[e] Alpha fetoprotein

[f] Des-γ-carboxy prothrombin

[g] Hyaluronic acid

[h] TNM; primary tumor/lymph node/distant metastasis

SELDI-TOF/MS analysis of sera

Expression difference mapping analysis profiles of the samples were obtained using weak cation-exchange (CM10) ProteinChip Arrays (Bio-Rad Laboratories). Arrays were analyzed by ProteinChip reader as previously reported [15]. In addition, the laser intensity ranged from 220 to 245, with a detector sensitivity of 8, and spectra ranging from 1300 to 150000 m/z were selected for analysis in this study.

Separation of candidate biomarker (8.1 k m/z)

The purification strategy was determined by the ProteinChip Arrays. Two hundred microliters of sera from HCV-HCC patients were diluted 5-fold into 50 mM Na-phosphate buffer, pH 7.0, and loaded onto a CM-Ceramic HyperD F spin column (Bio-Rad Laboratories). After equilibrating with the same buffer, the samples were eluted with a stepwise sodium chloride gradient from 0, 200, 300, and 1000 mM. The elution was desalinated and concentrated using a centrifugal concentrator (VIVA-SPIN, Vivascience, Hannover, Germany), and the purification progress was monitored using NP20 arrays. The flow-through fraction was dialyzed and then separated by 16.5% tricine one-dimensional sodium dodecyl sulfate–polyacrylamide gel electrophoresis (SDS–PAGE). The SDS–PAGE samples were run in tricine sodium dodecyl sulfate buffer according to the manufacturer's instructions and then stained with Coomassie brilliant blue (CBB).

Identification of the candidate biomarker (8.1 k m/z)

Gel pieces containing the target 8.1 k m/z protein were excised. The excised bands were reduced and alkylated for 30 min at room temperature, and then digested with trypsin (Modified Sequence Grade, Roche Diagnostics, Basel, Switzerland) in Tris–HCl, pH 8.0, for 20 h at 35°. The reaction solution was applied to NP20 arrays and allowed to air dry. To identify the protein, the digested peptides were purified by high-performance liquid chromatography (HPLC; MAGIC 2002; Michrom Bioresources Inc., Auburn, CA) and analyzed by Q-Tof2 (Micromass; Waters Ltd., Hertsfordshire, UK). The HPLC solvent consisted of solvent A (2% acetonitlile/0.1% formic acid) and B (90% acetonitlile/0.1% formic acid). The digested peptides were separated with a linear gradient from 10 to 50% solvent B with a flow rate of 400 nl/min using HPLC [19]. Mass spectral data were searched with Mascot (http://www.matrixscience.com) to identify proteins based on the peptide mass [20, 21].

Immunodepletion assay

For immunodepletion, serum samples were prepared as follows. Sera (250 μl) from HCC patients were diluted 5-fold in 50 mM Tris–HCl buffer, pH 8.0, and loaded onto a CM-Sepharose Fast Flow spin column (GE Healthcare Bio-Sciences Corp., NJ). After equilibration with the same buffer, the samples were eluted with a stepwise sodium chloride gradient from 0, 500, and 1000 mM. The elution from each NaCl concentration was monitored using NP20 arrays. To prepare the antibodies for immunodepletion, 6 μl anti-human C3 antibody, which detected C3 and C3a expression, or anti-C4a antibody (Santa Cruz Biotechnology, Santa Cruz, CA) was incubated with 20 μl Interaction Discovery Mapping (IDM) affinity beads (Bio-Rad Laboratories) and Protein A (Sigma Chemical Co, St. Louis, MO) over night at 4° with shaking. These beads were centrifuged, and the supernatant was discarded. The beads were washed with 50 mM phosphate buffer (pH 7.0), and 3 μl of the prepared serum sample was incubated with 15 μl IDM affinity beads with shaking for 2 h at 4°. As a negative control, 3 μl sample was incubated with IDM affinity beads and Protein A with an anti-C4a antibody or without antibody. After the incubation, the samples were cleared by centrifugation, and 5 μl of each supernatant was analyzed on NP20 ProteinChip arrays in a PBS II reader.

Cell culture and SELDI-TOF/MS analysis of culture supernatants

The human hepatocarcinoma cell line HuH-7 and human hepatoblastoma cell line HepG2 were cultured in Dulbecco's modified Eagle's medium supplemented with 10% fetal bovine serum (FBS), 100 IU/ml penicillin G, and 100 mg/ml streptomycin sulfate (Invitrogen, Carlsbad, CA). Before starting the experiments, the cells were cultured on 96-well microplates in medium without FBS for 24 h. After washing with FBS-free media, the cells were cultured for 24 h with FBS-free media with or without 500 μg/ml of C3a (Calbiochem, San Diego, CA). The supernatants were collected by centrifugation and analyzed for the expression of 8.1 k m/z using the ProteinChip system.

Statistical analysis

Values are shown as the means ± SD. Statistical differences, including laboratory data and individual peaks in SELDI TOF/MS, were determined using the Mann–Whitney U test. Values of $p < 0.05$ were considered statistically significant. The discriminatory power for each putative marker was described via receiver operating characteristics

(ROC) area under the curve (AUC). These statistical analyses were performed using STATVIEW 4.5 software (Abacus Concepts, Berkeley, CA), SPSS software (SPSS Inc., Chicago, IL), JMP software, or Ciphergen ProteinChip Software, version 3.0.2.

Results

Profiling sera from HCC patients and healthy controls

We analyzed the sera of all patients with HCV-HCC or HCV-CLD and healthy controls without HCC using the CM10 ProteinChip array to identity the most differential protein peak. Peaks were automatically detected using the Ciphergen ProteinChip Software 3.0.2. following baseline subtraction as described previously [15, 22]. This analysis identified 178 protein peak clusters, as seen in the spectrum representations from the three groups (HCV-HCC, HCV-CLD, and healthy control) in the 3000- to 15000-m/z range. Peak expressions were increased for 18 proteins and decreased for 14 proteins in sera from HCV-HCC patients compared to HCV-CLD patients. Compared to healthy subjects, 68 protein peaks were increased, and 16 protein peak intensities were decreased in the sera of HCV-HCC patients. Five protein peaks (4067, 4470, 7564, 7929, and 8130 m/z) had a p-value less than 1×10^{-7} and were significantly increased in the sera of HCC patients compared to the sera of HCV-CLD patients and healthy volunteers. In particular, an 8130 m/z peak was the most significantly different peak and had the most differential expression profile between patients with HCV-HCC and with HCV-CLD.

Purification and identification of the 8.1 k m/z peak

We optimized the adsorption and desorption conditions on the arrays using an HCV-HCC patient serum sample and healthy volunteer serum sample in order to determine a procedure to purify the target 8.1 k m/z protein. The optimal pH for retention of the 8.1 k m/z protein was a *pI* value of approximately 7.0 on the CM10 arrays, which indicates that weak cation-exchange sorbents and buffer pH should be fixed for further experiments. The target protein was eluted by increasing the sodium chloride concentrations in a Na-phosphate buffer and was eluted in the 1000 mM sodium chloride fraction. The concentrated serum protein that was eluted with 1000 mM sodium chloride was applied to SDS–PAGE for further separation. The 8.1 k m/z protein was identified and excised by in-gel trypsin digestion for identification. The peptide sequences were analyzed using liquid chromatography (LC)-MS/MS and then examined by a database search with Mascot. The digested peptides matched human complement C3a (Fig. 1).

After reacting the HCC sera with anti-complement C3a or anti-C4 antibodies or without antibody, the supernatants were analyzed by the SELDI ProteinChip system for immunodepletion. Analysis of the supernatant showed that only the 8.1 k m/z peak corresponding to complement C3a

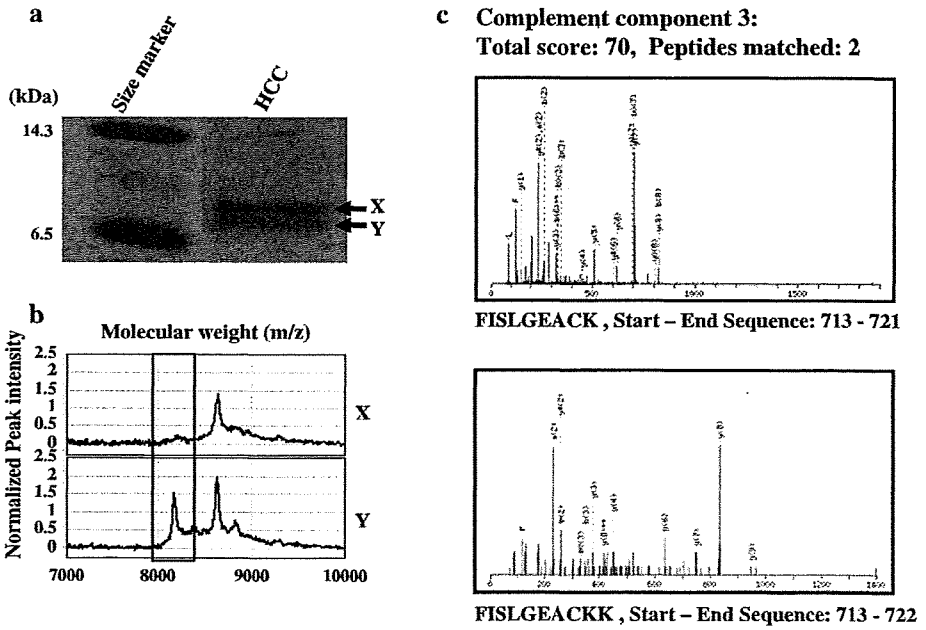

Fig. 1 **a** Partially purified proteins were separated by SDS–PAGE using serum samples from HCV-HCC patients. The Coomassie-stained SDS-PAGE gel shows two clear bands at approximately 8 kDa (*X* and *Y*). **b** After each band (*X* and *Y*) was excised from the gel, the proteins were extracted and analyzed using the ProteinChip system. The target protein in the excised band was detected, and the 8.1 k m/z peak corresponded only to the "*Y*" band contained in gel. **c** The excised "*Y*" band was alkylated and digested using trypsin. The peptides were collected and subjected to LC–MS/MS analysis. The proteins, which were derived from complement C3a, were identified using a database search

was reduced. On the other hand, immunodepletion with a control anti-C4 antibody or without antibody did not reduce the 8.1 k m/z peak (Fig. 2).

Profiling the C3a of sera from patients with HCC and without HCC

The 8.1 k m/z peak was confirmed as the complement C3a fragment using an immunodepletion assay. However, C3a was stabilized as C3adesArg with a molecular weight of approximately 8.9 k m/z. Figure 3a, b compares the expression of the 8.1 k m/z peak in the sera of HCV-HCC or HCV-CLD patients and healthy controls. The intensities

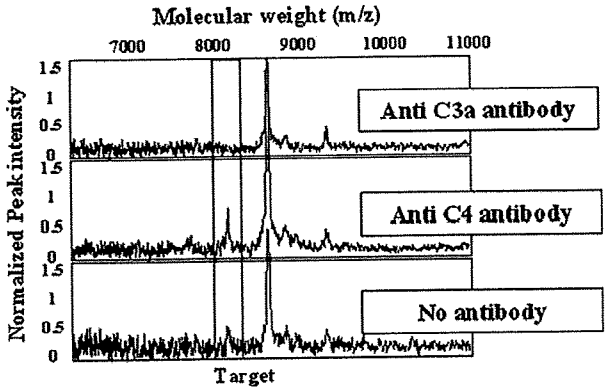

Fig. 2 Immunodepletion assay of the C3a fragment. Analysis of supernatant that had been immunodepleted with an anti-C3a antibody showed that only the 8.1 k m/z peak corresponding to complement C3a was reduced. Supernatants that had been immunodepleted with either a control anti-C4 antibody or without antibody did not have reduced 8.1 k m/z peaks by the ProteinChip system

in HCC patient sera were significantly higher than those in the HCV-CLD patients or healthy controls. The expression of the 8.9 k m/z peak in HCV-HCC patients was also higher than that in HCV-CLD patients or healthy controls (Fig. 3c, d). Although the 8.9 k m/z peak was not identified as C3adesArg, it is possible that both the 8.1 and 8.9 k m/z peaks were specific tumor markers for HCC. Furthermore, we analyzed sera from 10 HCV-HCC patients who were diagnosed with HCC within 1 or 2 years and sera from five patients who had received curative treatments using RFA, PEIT, and TACE for HCC. The 8.1 k m/z C3a fragment in the HCV-HCC patients was significantly increased in the year of disease onset compared to the pre-onset year. After treatment, expression of the C3a fragment significantly decreased in all five of the patients who had measurable samples after treatment (Fig. 4a). In contrast, the 8.9 k m/z peak did not change regardless of the occurrence of HCC over time (Fig. 4b). Thus, the 8.1 k m/z C3a fragment appears to be the most discriminatory tumor marker for HCV-HCC.

Relationship between the C3a fragment and other tumor markers

AFP and DCP levels were measured in sera from 83 of 87 patients with HCV-associated liver disease. The recommended cutoff levels for these tumor markers, AFP and DCP, are 20 ng/ml and 40 mAU/ml, respectively. AFP-L3 in 26 patients with HCV-associated liver disease was also investigated among measurable samples in which AFP in a total 35 patients was higher than 20 ng/ml. The cutoff level of AFP-L3 was set at 10%. When samples from patients

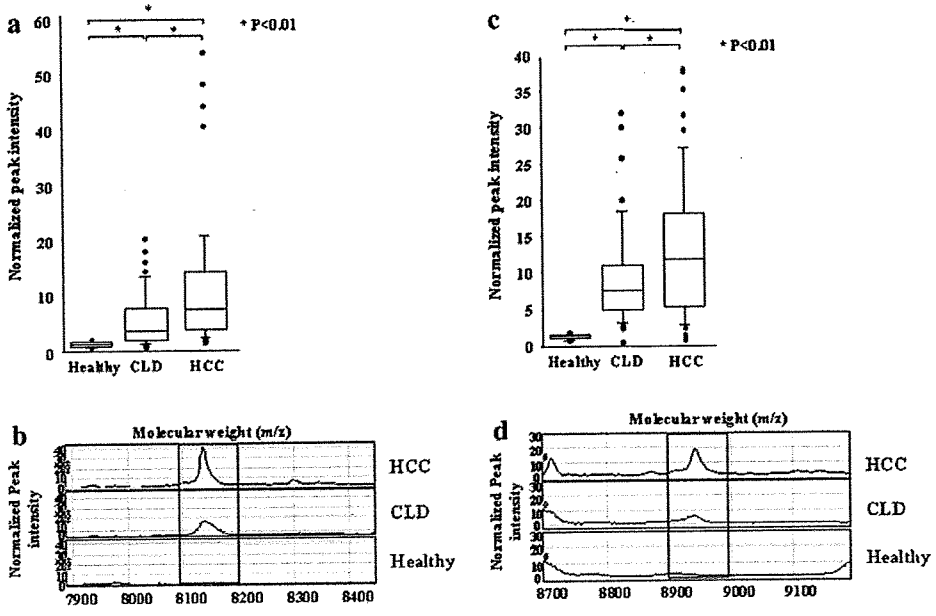

Fig. 3 **a** and **c** Comparisons of the expression profiles of the 8.1 and 8.9 k m/z peaks in HCV-HCC, HCV-CLD, and healthy sera. *Boxes* indicate the median ± 25th percentile. The *lower* and *upper bars* represent the 10th and 90th percentiles, respectively. **b** and **d** Representative spectra of the 8.1 and 8.9 k m/z peaks from patients in each group. The *horizontal axis* indicates the protein molecular weight, while the *vertical axis* designates the relative intensity

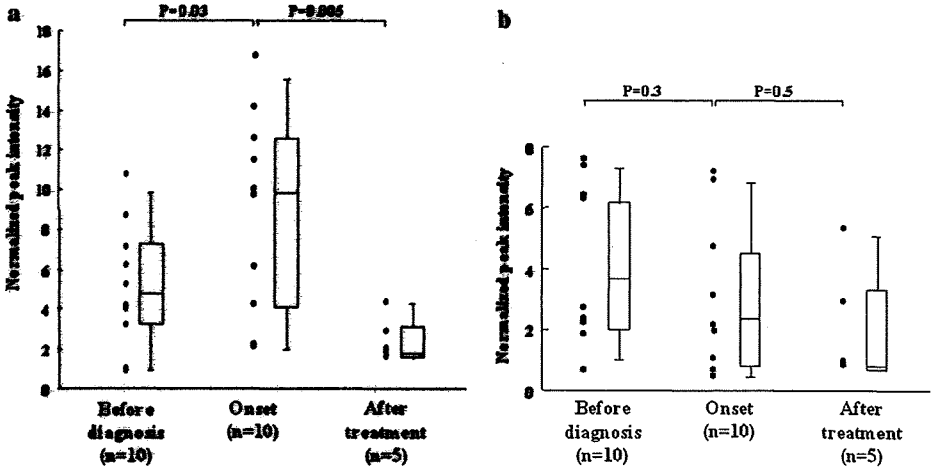

Fig. 4 Comparisons of the expression profiles of the 8.1 k m/z (**a**) and 8.9 k m/z (**b**) peaks in sera from HCV-HCC patients before diagnosis, during disease onset, and after treatment. The samples in the before diagnosis group included sera collected 1 or 2 years before the onset of HCC. *Boxes* indicate the median ± 25th percentile, the *lower bar* indicates the 10th percentile and the *upper bar* indicates the 90th percentile

Table 2 Diagnostic rates for hepatocellular carcinoma in the HCV infected patients

Markers	Sensitivity (%)	Specificity (%)	ROC AUC
AFP[a] (>20 ng/ml)	38 (17/45)	47 (18/38)	0.53
DCP[b] (>40 mAU/ml)	45 (20/44)	74 (29/39)	0.68
AFP-L3[c] (>10%)	58 (8/14)	50 (6/12)	0.58
C3a fragment (>3.5)	78 (37/45)	52 (22/42)	0.70
C3a fragment + AFP	91 (41/45)	26 (10/38)	0.72
C3a fragment + DCP	93 (41/44)	33 (13/39)	0.77
AFP + DCP	64 (28/44)	34 (12/35)	0.70
C3a fragment + AFP + DCP	98 (43/44)	20 (7/35)	0.80

[a] Alpha fetoprotein

[b] Des-γ-carboxy prothrombin

[c] Alpha fetoprotein, lectin lens culinaris agglutin-bound fraction

with HCV-HCC and HCV-CLD without HCC were compared, the sensitivity and specificity of AFP were 38 and 47%, whereas those of DCP were 45 and 74% and those of AFP-L3 were 58 and 50%, respectively. When the cutoff level for the relative intensity of the C3a fragment was set at 3.5, the sensitivity and specificity were 78 and 52%, respectively; the C3a fragment had the most sensitivity for the diagnosis of HCC. Furthermore, the ROC AUC of the C3a fragment, AFP, DCP, and AFP-L3 was 0.70, 0.53, 0.68, and 0.58, respectively (Table 2). There was no relationship between the C3a fragment and several other tumor and inflammation markers [AFP, DCP, AFP-L3, alanine aminotransferase (ALT), and high-sensitivity C-reactive protein (hs-CRP)], and each of these markers was independent of the diameter and number of tumors. The ROC AUC using AFP and DCP was highly similar to the ROC AUC with the C3a fragment alone. In addition, we investigated a combination assay that included the C3a fragment, AFP and DCP. This combination test, in which at least AFP, DCP, or the C3a fragment was positive, had a positive identification rate of 98%, although the specificity of this assay was too low at 20%. The ROC AUC of the combination test using AFP, DCP, and the C3a fragment was higher than those of any other markers. This result indicates that this combination assay using three markers is more useful than the combination assay using AFP ± DCP, which are measured worldwide to detect HCC (Table 2).

Profiling C3a expression in culture medium

C3a reacted with HCC cell lines, and the C3a peak in the culture medium was monitored by the ProteinChip system. The C3a fragment (approximately 8.1 k m/z) was not detected in the supernatants of HuH-7 and HepG2 cell cultures. However, the 8.9 k m/z peak was detected in the culture medium. This 8.9 k m/z peak was considered to be a stabilized form of C3a. This result indicated that the stabilized form of C3a (8.9 k m/z) was not undergoing proteasome-mediated degradation to yield the C3a fragment (8.1 k m/z) in these HCC cell lines.

Discussion

Because the HCC disease-associated mortality rate remains high, it is highly important to develop early diagnostic tools and treatments for HCC. Our study indicates that an 8.1 k m/z peak, which was identified as the C3a fragment by both peptide sequencing and an immunoassay, is up-regulated in the serum of HCC patients, 93% (42/45) of whom were TNM stage I or II. The C3a fragment in some HCC cases was also significantly higher in the year of HCC onset compared to the pre-onset year and decreased after curative treatment. Therefore, the C3a fragment appears to

be a promising simple tumor marker for the diagnosis of early HCC. In addition, a combination serum HCC diagnostic test that included AFP, DCP, and the C3a fragment had higher sensitivity than each individual marker. These results suggest that this combination test may be a useful HCC screening method, although the low specificity may pose challenges. Further examinations are needed to determine whether the C3a fragment or a combination test can be used to detect early HCC.

The results of our study demonstrated that the C3a fragment (8.1 k m/z) is a highly expressed novel tumor marker that is abundant in the sera of early HCC patients but not in the sera of healthy volunteers or HCV-CLD patients. A similar study by Lee et al. [17] used the ProteinChip SELDI system to show that C3a is a potential candidate biomarker for HCV-HCC. However, Lee et al. found that the molecular weight of C3a was represented by an approximately 8.9 k m/z peak. C3a has a very short half-life and is immediately cleaved into the more stable C3adesArg (8.9 k m/z), which is the anaphylatoxin C3a that lacks the C-terminal arginine and is stable state in the serum [23]. In our study, the 8.9 k m/z peak was also significantly different among HCV-HCC patients, HCV-CLD patients, and healthy volunteers (Fig. 3c, d). However, the discriminatory power of the 8.9 k m/z peak (ROC AUC was 0.60) was lower than the 8.1 k m/z peak (ROC AUC was 0.70) to distinguish between HCV-HCC and HCV-CLD. In addition, unlike the 8.1 k m/z peak, the levels of the 8.9 k m/z peak did not significantly increase with time as HCC progressed in 10 HCV-HCC cases (Fig. 4b). In contrast, Li et al. identified two proteins (8926 m/z and 8116 m/z) as complement component C3adesArg and a C-terminal truncated form of C3adesArg; the latter was a C-terminal truncation of C3adesArg that lacked the C-terminal sequence RASHLGLA (referred to as C3adesArgΔ8) in breast cancer patients [24]. However, these two biomarkers cannot be used to discriminate between breast cancers and benign tumors, and there were minimal differences in the peak intensities between breast cancer patients and healthy controls. Therefore, the C3a fragment with a molecular weight of 8.1 k m/z appears to be a potential diagnostic marker for HCC, although we cannot explain why the 8.1 k m/z fragment of C3a is overexpressed in HCC patients and did not confirm whether our C3a fragment (8.1 k m/z) is C3adesArgΔ8.

C3a, including C3adesArg, was also previously identified as a tumor marker for lymphoid malignancies, breast and colorectal cancers using the ProteinChip SELDI system [24–26]. Complement activation and subsequent deposition of complement components on tumor tissues has been demonstrated in cancer patients [27]. Malignant ovarian cells isolated from ascitic fluid samples had C3 activation products deposited on their cell surface [28]. Complement components are important mediators of inflammation and help regulate the immune response. C3a is biologically active and binds to mast cells and basophils, triggering the release of their vasoactive contents [29]. We investigated C3a expression by immunochemical examination of HCC tissues and Western blot analysis of proteins extracted from human HCC cell lines, including HepG2 and HuH-7. However, specific C3a expression, including the C3a fragment (8.1 k m/z), was not detected.

The complement system can be activated after exposure to tumor antigens [30]. It is speculated that small tumors can trigger a systematic reaction. Therefore, elevated C3a (8.9 k m/z) levels in the serum of HCV-HCC patients may reflect both a systematic immune response to HCV infection and non-specific tumor antigens rather than a specific immune response to HCC [24–26, 31]. In contrast, it is possible that overexpression of the C3a fragment (8.1 k m/z) is specific for HCC in addition to non-specific C3 activation.

In contrast to our results, Steel et al. [32] searched for HCC biomarkers using HCC-associated HBV-infected patient sera and found that the C-terminal fragment of complement C3 was down-regulated. Kawakami et al. [33] searched for characteristic alterations in the sera of HBV- and HCV-HCC-infected patients who had undergone curative radiofrequency ablation treatment and showed that C3 was up-regulated after treatment. In these studies, C3 was separated and identified using 2-DE of a mixture of proteins from a small number of patient sera samples, and this process identified various molecular weights for C3. In addition, we analyzed the sera of 25 patients with HCC-associated HBV infections, and the profile of several proteins was different between HCV- and HBV-infected patients. Although 35 protein peaks, including the C3a fragment, were overexpressed in the sera of both HCV-HCC and HBV-HCC patients compared to sera from healthy volunteers, the C3a fragment (8.1 k m/z) was particularly overexpressed in the sera of HCV-HCC patients and was not significantly different between HBV-HCC patients and HCV-CLD patients without HCC (data not shown). The biologic and pathogenic activities of HCV and HBV are different, and the molecular mechanisms underlying the development of hepatitis and hepatocarcinogenesis may differ between HBV and HCV infections [34–36]. Although the number of samples, cause of liver disease, and method of protein identification may affect these results, we speculate that the C3a fragment with a molecular weight of 8.1 k m/z is a candidate tumor marker for HCV-HCC but not HBV-HCC.

AFP, which is a commonly used HCC tumor marker, is elevated not only during HCC, but also during hepatocyte regeneration following liver damage. Previous reports revealed that AFP was abnormally elevated in the sera of patients with acute hepatitis, chronic hepatitis, and liver

cirrhosis. This lack of specificity for HCC means that AFP has a comparatively high false-positive rate [37]. The C3a fragment may also be elevated during hepatocyte regeneration following liver damage [38], and early diagnosis of small HCC tumors may be difficult with one marker alone. Therefore, the false-positive rates for HCC must be carefully considered [39–41]. Also, a combination of markers, including AFP, DCP, and the C3a fragment, in the serum should be verified to improve the diagnostic rate.

The ProteinChip SELDI system can separate and partially characterize multiple proteins in tissue and serum samples. Our previous report used a panel of proteins to diagnose early HCC with the ProteinChip SELDI system [15]. This panel diagnosis of seven protein peaks included a discriminant peak of 4060 m/z. This 4060 m/z peak may be a double-charged 8130 m/z peak, although the C3a fragment (8130 m/z) was not used to develop this diagnostic method. These results suggest that the C3a fragment is a useful HCC biomarker, regardless of whether this fragment carries a single or double charge. In addition, the panel diagnosis method is more useful than measuring the C3a fragment alone to diagnose and predict the occurrence of HCC. However, this method must be performed using the ProteinChip SELDI system, which is expensive and does not detect putative interactions between various proteins. Identifying a specific HCC protein such as the C3a fragment will also further our understanding of the molecular mechanisms of hepatocarcinogenesis. Therefore, the C3a fragment should not only be considered a simple HCC tumor marker, but should also be evaluated for its contribution to HCC carcinogenesis.

In conclusions, serum profiling with the ProteinChip SELDI system may be used to distinguish HCC from chronic liver disease without HCC and to detect early HCC in HCV-infected patients. Because we identified the C3a fragment (8.1 k m/z) in serum samples from HCC patients, the C3a fragment is a promising marker that can be used to screen for HCV-HCC and to develop new therapeutic targets.

Acknowledgments We thank Mr. Hiroyuki Nakao for assistance with the statistical analyses. We also thank Ms. Yuko Morinaga for her technical assistance. This work was supported in part by a grant-in-aid from the Collaboration of Regional Entities for the Advancement of Technological Excellence (CREATE) from the Japan Science and Technology Agency, a grant (no. CA87982) from the United States National Institutes of Health, and a grant-in-aid (Research on Hepatitis and BSE) from the Ministry of Health, Labour and Welfare of Japan.

References

1. El-Serag HB, Mason AC. Rising incidence of hepatocellular carcinoma in the United States. N Engl J Med. 1999;340:745–50.
2. Robert GG. Hepatocellular carcinoma: overcoming challenges in disease management. Clin Gastroenterol Hepatol. 2006;4:252–61.
3. Okuda K. Hepatocellular carcinoma. J Hepatol. 2000;32:225–37.
4. Oka H, Tamori A, Kuroki T, Kobayashi K, Yamamoto S. Prospective study of alpha-fetoprotein in cirrhotic patients monitored for development of hepatocellular carcinoma. Hepatology. 1994;19:61–6.
5. Ishii M, Gama H, Chida N, Ueno Y, Shinzawa H, Takagi T, et al. Simultaneous measurements of serum alpha-fetoprotein and protein induced by vitamin K absence for detecting hepatocellular carcinoma. South Tohoku District Study Group. Am J Gastroenterol. 2000;95:1036–40.
6. Okuda H, Nakanishi T, Takatsu K, Saito A, Hayashi N, Takasaki K, et al. Serum levels of des-gamma-carboxy prothrombin measured using the revised enzyme immunoassay kit with increased sensitivity in relation to clinicopathologic features of solitary hepatocellular carcinoma. Cancer. 2000;88:544–9.
7. Grazi GL, Mazziotti A, Legnani C, Jovine E, Miniero R, Gallucci A, et al. The role of tumor markers in the diagnosis of hepatocellular carcinoma, with special reference to the des-gamma-carboxy prothrombin. Liver Transpl Surg. 1995;1:249–55.
8. Wang CS, Lin CL, Lee HC, Chen KY, Chiang MF, Chen HS, et al. Usefulness of serum des-gamma-carboxy prothrombin in detection of hepatocellular carcinoma. World J Gastroenterol. 2005;11:6115–9.
9. Marrero JA, Su GL, Wei W, Emick D, Conjeevaram HS, Fontana RJ, et al. Des-gamma carboxyprothrombin can differentiate hepatocellular carcinoma from nonmalignant chronic liver disease in American patients. Hepatology. 2003;37:1114–21.
10. Mita Y, Aoyagi Y, Yanagi M, Suda T, Suzuki Y, Asakura H. The usefulness of determining des-gamma-carboxy prothrombin by sensitive enzyme immunoassay in the early diagnosis of patients with hepatocellular carcinoma. Cancer. 1998;82:1643–8.
11. Taketa K, Okada S, Win N, Hlaing NK, Wind KM. Evaluation of tumor markers for the detection of hepatocellular carcinoma in Yangon General Hospital, Myanmar. Acta Med Okayama. 2002;56:317–20.
12. Khien VV, Mao HV, Chinh TT, Ha PT, Bang MH, Lac BV, et al. Clinical evaluation of lentil lectin-reactive alpha-fetoprotein-L3 in histology-proven hepatocellular carcinoma. Int J Biol Markers. 2001;16:105–11.
13. Zinkin NT, Grall F, Bhaskar K, Otu HH, Spentzos D, Kalmowitz B, et al. Serum proteomics and biomarkers in hepatocellular carcinoma and chronic liver disease. Clin Cancer Res. 2008;14:470–7.
14. Schwegler EE, Cazares L, Steel LF, Adam BL, Johnson DA, Semmes OJ, et al. SELDI-TOF MS profiling of serum for detection of the progression of chronic hepatitis C to hepatocellular carcinoma. Hepatology. 2005;41:634–42.
15. Kanmura S, Uto H, Kusumoto K, Ishida Y, Hasuike S, Nagata K, et al. Early diagnostic potential for hepatocellular carcinoma using the SELDI ProteinChip system. Hepatology. 2007;45:948–56.
16. Paradis V, Degos F, Dargère D, Pham N, Belghiti J, Degott C, et al. Identification of a new marker of hepatocellular carcinoma by serum protein profiling of patients with chronic liver diseases. Hepatology. 2005;41:40–7.
17. Lee IN, Chen CH, Sheu JC, Lee HS, Huang GT, Chen DS, et al. Identification of complement C3a as a candidate biomarker in human chronic hepatitis C and HCV-related hepatocellular carcinoma using a proteomics approach. Proteomics. 2006;6:2865–73.
18. Uto H, Hayashi K, Kusumoto K, Hasuike S, Nagata K, Kodama M, et al. Spontaneous elimination of hepatitis C virus RNA in individuals with persistent infection in a hyperendemic area of Japan. Hepatol Res. 2006;34:28–34.
19. Shevchenko A, Wilm M, Vorm O, Mann M. Mass spectrometric sequencing of proteins silver-stained polyacrylamide gels. Anal Chem. 1996;68:850–8.
20. Prahalad AK, Hickey RJ, Huang J, Hoelz DJ, Dobrolecki L, Murthy S, et al. Serum proteome profiles identifies parathyroid hormone physiologic response. Proteomics. 2006;6:3482–93.

21. Shiwa M, Nishimura Y, Wakatabe R, Fukawa A, Arikuni H, Ota H, et al. Rapid discovery and identification of a tissue-specific tumor biomarker from 39 human cancer cell lines using the SELDI ProteinChip platform. Biochem Biophys Res Commun. 2003;309:18–25.
22. Adam BL, Qu Y, Davis JW, Ward MD, Clements MA, Cazares LH, et al. Serum protein fingerprinting coupled with a pattern-matching algorithm distinguishes prostate cancer from benign prostate hyperplasia and healthy men. Cancer Res. 2002;62: 3609–14.
23. Sahu A, Lambris JD. Structure and biology of complement protein C3, a connecting link between innate and acquired immunity. Immunol Rev. 2001;180:35–48.
24. Miguet L, Bogumil R, Decloquement P, Herbrecht R, Potier N, Mauvieux L, et al. Discovery and identification of potential biomarkers in a prospective study of chronic lymphoid malignancies using SELDI-TOF-MS. J Proteome Res. 2006;5:2258–69.
25. Ward DG, Suggett N, Cheng Y, Wei W, Johnson H, Billingham LJ, et al. Identification of serum biomarkers for colon cancer by proteomic analysis. Br J Cancer. 2006;94:1898–905.
26. Li J, Orlandi R, White CN, Rosenzweig J, Zhao J, Seregni E, et al. Independent validation of candidate breast cancer serum biomarkers identified by mass spectrometry. Clin Chem. 2005;51:2229–35.
27. Jurianz K, Ziegler S, Garcia-Schüler H, Kraus S, Bohana-Kashtan O, Fishelson Z, et al. Complement resistance of tumor cells: basal and induced mechanisms. Mol Immunol. 1999;36:929–39.
28. Bjørge L, Hakulinen J, Vintermyr OK, Jarva H, Jensen TS, Iversen OE, et al. Ascitic complement system in ovarian cancer. Br J Cancer. 2005;92:895–905.
29. Mollnes TE, Garred P, Bergseth G. Effect of time, temperature and anticoagulants on in vitro complement activation: consequences for collection and preservation of samples to be examined for complement activation. Clin Exp Immunol. 1988;73: 484–8.
30. Verhaegen H, De Cock W, De Cree J, Verbruggen F. Increase of serum complement levels in cancer patients with progressing tumors. Cancer. 1976;38:1608–13.
31. Habermann JK, Roblick UJ, Luke BT, Prieto DA, Finlay WJ, Podust VN, et al. Increased serum levels of complement C3a anaphylatoxin indicate the presence of colorectal tumors. Gastroenterology. 2006;131:1020–9.
32. Steel LF, Shumpert D, Trotter M, Seeholzer SH, Evans AA, London WT, et al. A strategy for the comparative analysis of serum proteomes for the discovery of biomarkers for hepatocellular carcinoma. Proteomics. 2003;3:601–9.
33. Kawakami T, Hoshida Y, Kanai F, Tanaka Y, Tateishi K, Ikenoue T, et al. Proteomic analysis of sera from hepatocellular carcinoma patients after radiofrequency ablation treatment. Proteomics. 2005;5:4287–95.
34. Honda M, Kaneko S, Kawai H, Shirota Y, Kobayashi K. Differential gene expression between chronic hepatitis B and C hepatic lesion. Gastroenterology. 2001;120:955–66.
35. Kim W, Oe Lim S, Kim JS, Ryu YH, Byeon JY, Kim HJ, et al. Comparison of proteome between hepatitis B virus- and hepatitis C virus-associated hepatocellular carcinoma. Clin Cancer Res. 2003;9:5493–500.
36. Koike K. Steatosis, liver injury, and hepatocarcinogenesis in hepatitis C viral infection. J Gastroenterol. 2009;44:82–8.
37. Lok AS, Lai CL. Alpha-fetoprotein monitoring in Chinese patients with chronic hepatitis B virus infection: role in the early detection of hepatocellular carcinoma. Hepatology. 1989;9:110–5.
38. Markiewski MM, Mastellos D, Tudoran R, DeAngelis RA, Strey CW, Franchini S, et al. C3a and C3b activation products of the third component of complement (C3) are critical for normal liver recovery after toxic injury. J Immunol. 2004;173:747–54.
39. Oka H, Kurioka N, Kim K, Kanno T, Kuroki T, Mizoguchi Y, et al. Prospective study of early detection of hepatocellular carcinoma in patients with cirrhosis. Hepatology. 1990;12:680–7.
40. Tanaka N, Horiuchi A, Yamaura T, Komatsu M, Tanaka E, Kiyosawa K. Efficacy and safety of 6-month iron reduction therapy in patients with hepatitis C virus-related cirrhosis: a pilot study. J Gastroenterol. 2007;42:49–55.
41. Tsamandas AC, Antonacopoulou A, Kalogeropoulou C, Tsota I, Zabakis P, Giannopoulou E, et al. Oval cell proliferation in cirrhosis in rats. An experimental study. Hepatol Res. 2007;37:755–64.

THE JOURNAL OF BIOLOGICAL CHEMISTRY VOL. 284, NO. 32, pp. 21165–21176, August 7, 2009

Proanthocyanidin from Blueberry Leaves Suppresses Expression of Subgenomic Hepatitis C Virus RNA*[S]

Received for publication, April 6, 2009, and in revised form, June 12, 2009 Published, JBC Papers in Press, June 16, 2009, DOI 10.1074/jbc.M109.004945

Masahiko Takeshita[‡], Yo-ichi Ishida[§], Ena Akamatsu[§], Yusuke Ohmori[¶], Masayuki Sudoh[¶], Hirofumi Uto[‖], Hirohito Tsubouchi[‖], and Hiroaki Kataoka[1]**

*From the [‡]Research Division, Minami Nippon Dairy Co-op Co., Ltd., Miyazaki 885-0073, the [§]Miyazaki Prefectural Industrial Support Foundation, Miyazaki 880-0303, the [¶]Kamakura Research Laboratories, Chugai Pharmaceutical Co., Ltd., Kanagawa 247-8530, the [‖]Department of Digestive Disease and Life-style Related Disease, Health Research Human and Environmental Sciences, Kagoshima University, Graduate School of Medicine and Dental Sciences, Kagoshima 890-8520, and the **Section of Oncopathology and Regenerative Biology, Department of Pathology, Faculty of Medicine, University of Miyazaki, Miyazaki 889-1692, Japan*

Hepatitis C virus (HCV) infection is a major cause of chronic liver disease such as chronic hepatitis, cirrhosis, and hepatocellular carcinoma. While searching for new natural anti-HCV agents in agricultural products, we found a potent inhibitor of HCV RNA expression in extracts of blueberry leaves when examined in an HCV subgenomic replicon cell culture system. This activity was observed in a methanol extract fraction of blueberry leaves and was purified by repeated fractionations in reversed-phase high-performance liquid chromatography. The final purified fraction showed a 63-fold increase in specific activity compared with the initial methanol extracts and was composed only of carbon, hydrogen, and oxygen. Liquid chromatography/mass-ion trap-time of flight analysis and butanol-HCl hydrolysis analysis of the purified fraction revealed that the blueberry leaf-derived inhibitor was proanthocyanidin. Furthermore, structural analysis using acid thiolysis indicated that the mean degree of polymerization of the purified proanthocyanidin was 7.7, consisting predominantly of epicatechin. Proanthocyanidin with a polymerization degree of 8 to 9 showed the greatest potency at inhibiting the expression of subgenomic HCV RNA. Purified proanthocyanidin showed dose-dependent inhibition of expression of the neomycin-resistant gene and the NS-3 protein gene in the HCV subgenome in replicon cells. While characterizing the mechanism by which proanthocyanidin inhibited HCV subgenome expression, we found that heterogeneous nuclear ribonucleoprotein A2/B1 showed affinity to blueberry leaf-derived proanthocyanidin and was indispensable for HCV subgenome expression in replicon cells. These data suggest that proanthocyanidin isolated from blueberry leaves may have potential usefulness as an anti-HCV compound by inhibiting viral replication.

Hepatitis C virus (HCV)[2] is often associated with the development of chronic liver diseases. Infection by HCV causes chronic hepatitis at high rates and finally results in liver cirrhosis and subsequent occurrence of hepatocellular carcinoma (1–3). The number of people worldwide who are infected by HCV is estimated to be over 200 million with 2 million infections in Japan (4). The South Kyushu area of Japan, including Miyazaki prefecture, has a high prevalence of this virus, and it is now recognized as a social problem. There is no vaccine effective for HCV at present. The elimination of HCV may be achieved by a combination of pegylated α-interferon and ribavirin, a broad spectrum antiviral drug (4–6). However, virological response to this combination therapy has been reported to be 80% for genotypes 2 and 3, but less than 50% for genotype 1 (7, 8). Moreover, α-interferon is associated with severe side-effects, including leucopenia, thrombocytopenia, depression, fatigue, and flu-like symptoms, and ribavirin is associated with side-effects such as hemolytic anemia (9). Therefore, establishment of a new modality of treatment without serious adverse effects is still required.

Considering the prolonged period (20–30 years) required for development of liver cirrhosis and hepatocellular carcinoma in individuals infected with HCV, we speculated that progression of the disease might be influenced by daily diet. Our research project focuses on the daily use of agricultural products that could cure or reduce the risk of disease progression by HCV. Thus, we screened local agricultural products (1700 samples from 283 species) for their suppressive activity against HCV subgenome expression using an HCV replicon cell system. We found a significant suppressive activity in extracts of blueberry leaves. Blueberries are classified in the genus *Vaccinium*, and the species are native only to North America. Blueberry leaves have high quinic acid and chlorogenic acid contents and also significant flavonol glycosides such as rutin. Thus, they are high in antioxidant activity. In our subsequent screening studies using various kinds of blueberry species, the most potent activity was observed in the leaf of rabbit-eye blueberry (*Vaccinium virgatum* Aiton), which is cultivated in southern areas of Japan.

* This study was supported by a grant from the Collaboration of Regional Entities for the Advancement of Technological Excellence (CREATE) from Japan Science and Technology Agency.

[S] The on-line version of this article (available at http://www.jbc.org) contains supplemental Figs. S1–S3.

[1] To whom correspondence should be addressed: Section of Oncopathology and Regenerative Biology, Dept. of Pathology, Faculty of Medicine, University of Miyazaki, 5200 Kihara, Kiyotake, Miyazaki 889-1692, Japan. Tel.: 81-985-85-2809; Fax: 81-985-85-6003; E-mail: mejina@fc.miyazaki-u.ac.jp.

[2] The abbreviations used are: HCV, hepatitis C virus; hnRNP, heterogeneous nuclear ribonucleoprotein; HPLC, high-performance liquid chromatography; PDA, photodiode array; EPMA, electron probe micro-analysis; LC/MS-IT-TOF, liquid chromatography/mass spectrometry-ion trap-time of flight; APCI, atmospheric pressure chemical ionization; mDP, mean degree of polymerization; IC_{50}, concentration required for 50% inhibition; CC_{50}, concentration required for 50% cytotoxicity; eIF3, eukaryotic translation initiation factor 3; CHAPS, 3-[(3-cholamidopropryl)dimethylammonio]-1-propane sulfonate; IRES, internal ribosome entry site; DIGE, differential gel electrophoresis.

In this study, extracts of rabbit-eye blueberry leaves were used in an effort to purify and identify the compound responsible for inhibition of the expression of subgenomic HCV RNA. We identified oligomeric proanthocyanidin with mean degree of polymerization (mDP) around eight as an inhibitor of HCV subgenome expression. We also analyzed cellular proteins that have affinity to the oligomeric proanthocyanidin in HCV replicon cells and identified heterogeneous nuclear ribonucleoprotein (hnRNP) A2/B1 as one of candidate proteins involved in the proanthocyanidin-mediated inhibition of HCV subgenome expression.

EXPERIMENTAL PROCEDURES

Extraction of Blueberry Leaves—A lyophilized powder made from leaves of rabbit-eye blueberry (*V. virgatum* Aiton) was provided by Unkai Shuzo Co., Ltd. (Miyazaki, Japan). One gram of the lyophilized powder was extracted with 100 ml of methanol at room temperature with shaking for 15 min, and the supernatant was passed through filter paper (filter paper No.2, Toyo, Tokyo, Japan). The methanol extract was then extracted with 100 ml of chloroform, followed by centrifugation (1750 × *g* for 10 min), and the resultant precipitate and supernatant were collected. The precipitate was dissolved in methanol, concentrated *in vacuo*, and lyophilized (CMW-ppt). The supernatant was mixed with 150 ml of distilled water and methanol to perform a liquid-liquid extraction, and the water layer was collected and mixed with 150 ml of chloroform to repeat the chloroform extraction. The water layer was concentrated and lyophilized (CMW-W). The chloroform layer was also concentrated and lyophilized (CMW-C). Most HCV subgenome-expression inhibitory activity was recovered in the CMW-W fraction.

Preparative Fractionation by HPLC—To separate the components in the CMW-W fraction processing inhibitory activity against HCV RNA expression, we performed HPLC (Prominence System, Shimadzu, Kyoto, Japan). Preliminary fractionation of CMW-W to confirm the elution pattern of HCV expression suppressive components was carried out on a reversed-phase column (Atlantis dC18, 4.6 mm × 150 mm, 3 μm, Waters, Milford, MA) at 40 °C with UV detection at 254 nm. A gradient consisting of eluant A (0.05% trifluoroacetic acid) and eluant B (acetonitrile) was applied at a flow rate of 0.7 ml/min as follows: 15–25% B linear from 0 to 12.5 min, 25–100% B linear from 12.5 to 17.5 min followed by washing 100% B from 17.5 to 25 min. For purification, the first HPLC fractionation was performed on a reversed-phase column (Atlantis T3, 4.6 mm × 150 mm, 3 μm, Waters). A gradient consisting of eluant A and eluant B (acetonitrile) was applied at a flow rate of 0.7 ml/min as follows: 30% B from 0 to 7.5 min, 30–100% B linear gradient from 7.5 to 12.5 min, followed by washing with 100% B from 12.5 to 20 min. The CMW-W fraction dissolved in 30 ml of methanol was injected, and the eluted fractions (2.1 to 18.0 min, total 26 fractions) were collected. The gradient program for the second fractionation was 20% B from 0 to 7.5 min, 20–100% B linear from 7.5 to 12.5 min, followed by washing with 100% B from 12.5 to 20 min. Fractionation of the eluate was the same as the first HPLC program. In the third HPLC fractionation, the eluant B was replaced by methanol and eluted with 40–65% B linear gradient from 0 to 12.5 min and 65–100% B linear gradient from 12.5 to 17.5 min. Fractions eluted from 2.2 to 17.5 min (total 26 fractions) were collected. In all experiments, suppressive activity of each fraction against HCV RNA expression was measured using replicon cells.

HCV Replicon Cells and Replicon Assay—The Huh-7/3-1 cell line carrying an HCV-replicon was used (10). The line was established from Huh-7 cells by stable transfection with subgenomic selectable RNA in which the encoding HCV structural proteins were replaced by the firefly luciferase gene, the internal ribosome entry site (IRES) of the *Encephalomyocarditis* virus and the neomycin phosphotransferase gene. With this HCV subgenome, the efficiency of subgenomic HCV expression could be estimated by measuring luciferase activity in the replicon cells. The HCV replicon cells were routinely grown in Dulbecco's modified Eagle's medium supplemented with Glutamax (Invitrogen), 10% fetal bovine serum, 1% penicillin/streptomycin (Invitrogen), and 500 μg/ml G418 (Invitrogen). Cells were maintained at 37 °C in a humidified atmosphere containing 5% CO_2. For the HCV subgenome expression assay, the replicon cells in Dulbecco's modified Eagle's medium supplemented with Glutamax and 5% fetal bovine serum were seeded in 96-well plates (5000 cells/well) and incubated for 24 h. Then the cells were cultured with various concentrations of samples for 72 h. Quantification of the luciferase activity was performed using the Steady-Glo Luciferase Assay System (Promega, Madison, WI) according to the manufacturer's instructions, and the luminescence was measured by DTX 800 Multimode Detector (Beckman Coulter, Fullerton, CA). The inhibitory activity was expressed as the concentration required for 50% inhibition (IC_{50}). Specific activity was calculated as a reciprocal number of IC_{50} ($1/IC_{50}$). Total activity was calculated by multiplying yielded weight by specific activity.

The cytotoxicity of the samples was measured by Cell Counting Kit-8 (Dojindo Molecular Technologies, Kumamoto, Japan) according to the manufacturer's instructions. Briefly, 10 μl/well of Cell Counting Kit-8 reagent was added to the cells cultured in a 96-well plate, incubated at 37 °C for 60 min. The absorbance of each well was measured at 450 nm with a reference wavelength at 650 nm using an Emax Precision microplate reader (Molecular Devices Inc., Sunnyvale, CA). Cell viability was calculated as relative index of control cells, and effects of samples on cell viability were expressed as the concentration required for 50% cytotoxicity (CC_{50}).

Constitutive Analysis of Electron Probe Micro-analysis and Liquid Chromatography/Mass Spectrometry-ion Trap-time of Flight (LC/MS-IT-TOF)—For electron probe micro-analysis (EPMA-1600, Shimadzu), the excitation voltage and the beam current were kept at 15 kV and at 100 nA, respectively. The diameter of the electron beam was 50 μm, and the sample was processed for carbon shadowing in advance.

Identification of the anti-HCV compound purified from blueberry leaves was done by HPLC-MSn fragmentation analyses. An HPLC System (Prominence System, Shimadzu) on a reversed-phase column (Atlantis T3, 2.1-mm inner diameter × 100 mm, 3 μm, Waters) was equipped with a photodiode array (PDA) detector scanning from 200 to 800 nm and mass spectrometry-ion trap-time of flight (MS-IT-TOF, Shimadzu)

detector. The mobile phase consisted of a gradient system 30 min of eluant A (0.05% trifluoroacetic acid) and eluant B (acetonitrile) at a flow rate of 0.25 ml/min. The elution program was 10–25% B linear from 0 to 7.5 min, 25–100% B linear from 7.5 to 12.5 min, followed by washing 100% B from 12.5 to 20 min. The column was maintained at 40 °C. Electrospray ionization conditions were recorded from m/z = 200 to 1500 in a negative ionization mode. Other MS conditions were as follows: interface voltage, −3.5 or −3.0 kV; nebulizer N_2 gas, 1.5 or 2.0 liters/min; drying N_2 pressure, 200 or 70 kPa, respectively. Heat block temperature and curved desolvation line temperature were both 200 °C. Analytical conditions were recorded from m/z 250 to 1500 in a negative ionization mode. Atmospheric pressure chemical ionization (APCI) probe temperature was set from 250 to 450 °C.

Analysis of Proanthocyanidin—Proanthocyanidins were characterized by a modified method of Porter *et al.* (11, 12), in which they were degraded to anthocyanidins by heating under acidic conditions. Briefly, 200 μl of purified compound from blueberry leaves (0.1–2.5 mg/ml) was mixed with 750 μl of *n*-butanol/HCl (95:5) and 50 μl of 1% of $NH_4Fe(SO_4)_2{\cdot}12H_2O$ dissolved in 2 M HCl. The mixture was vortexed and heated in an oven at 105 °C for 40 min, and cooled in flowing water. Optical densities of the treated solution were recorded at 540 nm by spectrophotometer (UV-1700, Shimadzu). Procyanidin B2 (Sigma-Aldrich) was used as a standard. The hydrolysates generated by the modified Porter method were also analyzed using LC/MS-IT-TOF as described above. The elution program was 10–40% B linear from 0 to 15 min followed by washing 100% B from 15 to 22.5 min. Electrospray ionization conditions were recorded from m/z 200 to 1500 in a positive ionization mode. Interface voltage and nebulizer N_2 were 4.5 kV and 1.5 L/min, respectively. MS/MS conditions were set to auto system and recorded from m/z 50 to 1000. The parent MS was searched from m/z 200 to 1500, and ion accumulation was 30 ms. The data were analyzed by LCMS solution v3.41 software and Formula Predictor Software (Shimadzu).

Thiolysis Analysis—Thiolysis was performed by a previously described method (13, 14) with some modifications. Briefly, 50 μl of purified samples (2 mg/ml in methanol) was mixed with 50 μl of methanol acidified with HCl (3.3%) and 100 μl of benzyl mercaptan (5% in methanol). The reaction was carried out at 50 °C for 30 min and then kept at ambient temperature for 3 h. Pure catechin or epicatechin solution (1.25 mg/ml in methanol) (Funakoshi, Tokyo, Japan) was also thiolyzed to obtain the epimerization rate to calculate the ratio of catechin and epicatechin in the terminal units. The reaction mixture was diluted 5-fold with methanol and analyzed by reverse-phase HPLC. An Atlantis T3 column (4.6 mm × 150 mm, 3 μm, Waters) was used at 40 °C as described above. UV detection was performed at 280 nm. The gradient program was 15–25% B linear from 0 to 10 min, 25–100% B linear from 10 to 30 min, followed by washing 100% B from 30 to 37.5 min and re-equilibration of the column 37.5 to 45 min under initial gradient conditions. To ascertain the elution pattern of thiolysis media and to estimate unknown peaks, LC/MS-IT-TOF was also employed in a negative ion mode. Flavan-3-ols and their benzylthio adducts obtained by thiolysis media of procyanidin B2 were used as a standard. The mDP was calculated by the formula, mDP = [sum of (benzylthio adducts × n) + sum of (free flavan-3-ol × n)]/[total free flavan-3-ol], in which "n" is DP of detected flavan-3-ol by thiolysis.

Preparation of Proanthocyanidin from Blueberry Leaves—To prepare proanthocyanidin from blueberry leaves, freeze-dried powder (100 g) was extracted with 1.2 liters of acetone for 10 min, and the supernatant was decanted. This procedure was repeated five times to remove the green pigment from the leaves, followed by washing in 1.2 liters of hexane for 30 min. The remaining residues were washed with ethyl acetate. The washed powder of leaves was extracted with 1.2 liters of methanol for 30 min, and the supernatant was filtered. This procedure was repeated four times, and the resulting crude methanol extracts were concentrated by rotary evaporator at 50 °C and lyophilized, finally resulting in ~30 g of solid powder. The crude methanol extract (15 g) was then dissolved in 1.0 liter of 60% methanol and placed on a Sephadex LH-20 column (50 mm × 920 mm, Amersham Biosciences). Fractionation was performed using the following series of solvents: fraction I, 9.0 liters of 60% methanol (retrieved weight: 10.2 g); fraction II, 9.0 liters of 100% methanol (retrieved weight: 3.3 g); fraction III, 9.0 liters of 70% (v/v) acetone (retrieved weight: 1.3 g). The LC/MS-IT-TOF analyses of each fraction indicated that fraction I was primarily composed of quinic acid, chlorogenic acid, and flavonol glycosides such as rutin. Fraction II consisted of proanthocyanidin oligomers from tetramer to decamer as analyzed by thiolysis. Fraction III consisted of proanthocyanidin polymers that were decamers or greater. In each fraction, the eluate was divided into 28 subfractions/liter.

Northern Blot Analysis—Total RNAs from cultured replicon cells were prepared using RNeasy mini kits (Qiagen). RNAs were denatured at 65 °C for 15 min, cooled on ice, and then separated by 1% agarose-formaldehyde gel electrophoresis (2 μg/lane) and transferred to a positively charged nylon membrane (Hybond-N^+, Amersham Biosciences). The membrane was hybridized with a biotinized probe of the neomycin phosphotransferase gene. For detection of the bound probe, membranes were incubated with streptavidin-Alexa Fluor 680 conjugate (Invitrogen), and the bound fluorescence was detected by Odyssey Infrared Imaging System (LI-COR Biosciences). For internal control, β-actin mRNA-specific biotinized antisense RNA probe was used.

Western Blot Analysis—Cultured replicon cells were harvested, and total cellular proteins were extracted with Cel-Lytic-M (Sigma-Aldrich) containing 1% protease inhibitor mixture (Sigma-Aldrich). The samples were separated by SDS-PAGE using 10% gel under reducing conditions. The proteins were transferred electrophoretically to an Immobilon-P membrane (Millipore, Bedford, MA).

The membrane was treated with a blocking buffer for near infrared fluorescent Western blotting (Rockland, Gilbertsville, PA). Primary antibodies used were anti-human hnRNP A2/B1, hnRNP K, hnRNP L, and hnRNP Q and anti-human β-actin antibodies (EF-67, D-6, A-11, 18E4, and I-19, respectively, Santa Cruz Biotechnology, Santa Cruz, CA), anti-human eukaryotic translation initiation factor 3 (eIF3) F, eIF3G eIF3H polyclonal antibodies (Novus Biologicals, Littleton, CO), and

anti-HCV NS-3 polyclonal antibody (10). The labeled proteins were visualized with Alexa Fluor 680 anti-rabbit or anti-mouse IgG (Invitrogen) or IRDye™ 800CW anti-goat IgG (LI-COR Biosciences) and detected by using as Odyssey Infrared Imaging System.

Affinity Purification of Proanthocyanidin-binding Proteins—Purified blueberry leaf-derived proanthocyanidin or catechin was coupled with epoxy-activated Sepharose 6B (Amersham Biosciences) according to the manufacturer's instructions. Approximately 5×10^8 HCV replicon cells were extracted with lysis buffer (50 mM sodium phosphate (pH 7.5), 1% CHAPS, 5 mM EDTA, 150 mM NaCl, and protease inhibitor mixture (Complete™, Roche Diagnostics, Mannheim, Germany)). The total protein extract (90 mg) was added to the coupled Sepharose beads (3 ml) and incubated at 4 °C overnight with gentle rotation. The beads were centrifuged ($500 \times g$) for 1 min, and the pellet was washed six times with the lysis buffer. The absorbed proteins were eluted by incubation in 2% SDS with 50 mM dithiothreitol at 100 °C for 10 min. The eluate was concentrated with an Amicon Ultra-4 Ultracel-5k (Millipore), and the solvent was replaced by the lysis buffer. Protein concentration was determined by the *o*-phthalaldehyde method using bovine serum albumin as the standard.

Fluorescent Two-dimensional DIGE—Fluorescent two-dimensional-DIGE was performed using fluorescent dyes, IC3-OSu and IC5-OSu (Dojindo Molecular Technologies), with a modification of the methods reported elsewhere (15, 16). Briefly, 10 μg of proteins per gel were precipitated using a two-dimensional clean-up kit (Bio-Rad) and then dissolved in 20 μl of sample buffer (10 mM sodium phosphate (pH 8.0), 7 M urea, 2 M thiourea, 3% CHAPS, and 1% Triton X-100). After addition of 400 pmol of IC3-OSu or IC5-OSu, proteins were incubated at 40 °C for 30 min. The labeling reaction was quenched by incubation with 400 μM lysine for 15 min, followed by addition of an equal volume of the sample buffer with 150 mM dithiothreitol, 0.4% Bio-Lyte 3–10 (Bio-Rad Laboratories), and 0.004% bromphenol blue. Two-dimensional gel electrophoresis was performed according to the manufacturer's instructions (Bio-Rad). The mixed samples were applied to ReadyStrip IPG strips (pH 3–10 NL, 7 cm, Bio-Rad) for separation in the first dimension. The second-dimensional separation was performed by SDS-PAGE using an 8% gel. Fluorescence imaging was performed on a Proxpress™ proteomic imaging system (PerkinElmer Life Sciences). IC3-OSu-labeled proteins were detected with 540/25 nm excitation and 590/35 nm emission filters. IC5-OSu-labeled proteins were detected with 625/35 nm excitation and 680/30 nm emission filters. In this study, while proteins from proanthocyanidin- or catechin-coupled Sepharose were labeled with IC5-OSu, a mixture of equal quantities of both samples was labeled with IC3-OSu and used as a reference for quantitation of IC5-OSu-labeled proteins as described (16). The fluorescent images were aligned using SameSpot TT900 S2S (Nonlinear Dynamics, Newcastle, UK) and then analyzed with Progenesis Discovery software (Nonlinear Dynamics). Each group (eluate from proanthocyanidin- or catechin-coupled Sepharose) was run on triplicate gels three times. Spot intensity in the IC5-OSu image was normalized to the intensity of the corresponding IC3-OSu image spot in the same gel. The average spot intensities ± standard deviation (S.D.) from nine gels were calculated. Statistical differences were determined by Student's *t* test, and *p* values <0.05 were considered significant. The proteins having high affinity to proanthocyanidin but not to catechin were detected using a 1.5-fold change ($p < 0.05$) as the cut off.

Protein Identification—Protein identification by peptide mass fingerprinting was performed as described previously (17). Briefly, 100 μg of proteins was separated by two-dimensional-DIGE gels and stained with Coomassie Brilliant Blue R-250. Protein spots of interest were excised from the gel and digested overnight with trypsin. Each peptide extract was deposited onto a thin layer of α-cyano-4-hydroxycinnamic acid (Bruker Daltonics, Bremen, Germany) and allowed to adsorb for 5 min, after which the layers were washed twice with 0.1% trifluoroacetic acid. Spectra were obtained using matrix-assisted laser desorption/ionization-TOF-TOF-MS, Autoflex II TOF/TOF (Bruker Daltonics) in positive-ion and reflectron mode. The data set was entered in an in-house Mascot search engine (Matrix Science, London, UK), to find the closest match with known proteins registered in the data base from the Swiss-Prot.

Knockdown of Proanthocyanidin-binding Proteins Using siRNAs—ON-TARGETplus SMARTpools of duplex siRNAs targeting hnRNP L, hnRNP K, hnRNP A2/B1, hnRNP A/B, hnRNP Q, eIF3F, eIF3G, eIF3H, and non-targeting control siRNA were purchased from Dharmacon (Thermo Fisher Scientific, Tokyo, Japan). Individual sequence of hnRNP A2/B1 siRNAs was confirmed by two single siRNAs (Target #09: 5′-CGGUGGAAAUUUCGGACCA-3′, Target #11: 5′-GGAGAGUAGUUGAGCCAAA-3′). The replicon cells were transfected with each siRNA using Lipofectamine RNAiMAX reagent (Invitrogen) according to the manufacturer's protocol. After 72 h incubation, the cells were assayed.

RESULTS

Purification of an Inhibitor of HCV Subgenome Expression from Blueberry Leaves—We screened 283 species of local agricultural products for their suppressive activity against the expression of subgenomic HCV RNA using an HCV replicon cell system, and found significant suppressive activity in the leaves of the blueberry (*Vaccinium virgatum* Aiton), peels of roots of Taro (*Colocasia esculenta* L.), and hulls of seeds of Japanese plum (*Prunus mume* Sieb. *et* Zucc). Among them, extracts of blueberry leaves contained the highest total activities. Therefore, we purified a compound from blueberry leaves that inhibited expression of subgenomic HCV RNA in replicon cells. An overall purification scheme is shown in Fig. 1, and a summary of the purification steps is shown in Table 1. From 1000 mg of lyophilized powder from the leaves, 440 mg of methanol extracts was obtained. The IC_{50} value of the methanol extracts was 5.47 μg/ml. The inhibitory activity was recovered in the CMW-W fraction (284.2 mg), in which the IC_{50} value was 1.74 μg/ml. The specific activity of CMW-W was 3-fold greater than that of the initial methanol extracts and the yield of the activity exceeded 200%, suggesting that an interfering substance had been removed.

The CMW-W fraction was subjected to a subsequent HPLC purification step in which a preliminary HPLC elution pattern